Article:
Peys, A., Isteri, V., Yliniemi, J. et al. (2022) Sustainable iron-rich cements: Raw material sources and binder types. Cement and Concrete Research, 157. 106834. ISSN: 0008-8846

https://doi.org/10.1016/j.cemconres.2022.106834

Cement and Concrete Research 157 (2022) 106834

Contents lists available at ScienceDirect

Cement and Concrete Research

journal homepage: www.elsevier.com/locate/cemconres

Sustainable iron-rich cements: Raw material sources and binder types

Arne Peys [a], Visa Isteri [b], Juho Yliniemi [c], Antonia S. Yorkshire [d], Patrick N. Lemougna [e,f], Claire Utton [d], John L. Provis [d], Ruben Snellings [a], Theodore Hanein [d,*]

[a] Sustainable Materials, VITO, Boeretang 200, 2400 Mol, Belgium
[b] Process metallurgy, Faculty of Technology, University of Oulu, PO Box 4300, 90014, Finland
[c] Fibre and Particle Engineering, Faculty of Technology, University of Oulu, PO Box 4300, 90014, Finland
[d] Department of Materials Science and Engineering, The University of Sheffield, Sheffield S1 3JD, UK
[e] Department of Materials and Chemistry, Vrije Universiteit Brussel, Pleinlaan 2, 1050 Brussels, Belgium
[f] Department of Minerals Engineering, School of Chemical Engineering and Mineral Industries (EGCIM), University of Ngaoundere, P.O. Box 454, Ngaoundere, Cameroon

ARTICLE INFO

Keywords:
Cement
Iron
Ferrite
Residue valorisation
Low-carbon
Clinkers
Supplementary cementitious materials
Alkali-activated materials

ABSTRACT

The bulk of the cement industry's environmental burden is from the calcareous source. Calcium is mostly available naturally as limestone ($CaCO_3$), where almost half of the mass is eventually released as CO_2 during clinker manufacture. Iron (Fe) is the fourth most common element in the Earth's crust surpassed only by oxygen, silicon, and aluminium; therefore, potential raw materials for alternative cements can contain significant amounts of iron. This review paper discusses in detail the most abundantly available Fe-rich natural resources and industrial by-products and residues, establishing symbiotic supply chains from various sectors. The discussion then focusses on the impact of high iron content in clinker and on ferrite (thermo)chemistry, as well as the importance of iron speciation on its involvement in the reactions as supplementary cementitious material or alkali-activated materials, and the technical quality that can be achieved from sustainable Fe-rich cements.

1. Introduction

The Earth's crust is composed of ~7 wt% iron (Fe), expressed as Fe_2O_3, which is only surpassed by oxygen (O), silicon (Si), and aluminium (Al) [1,2]. Iron itself is a key commodity and it is geochemically associated with many other economically important ores of base metals, such as Zn, Ni, Pb, Al, and Ti. Many extracted natural resources, industrial by-products and process residues are therefore rich in iron. As the world desperately needs a decrease in CO_2 output from anthropogenic activities, the construction industry is in pursuit of alternatives to its largest source of CO_2 emissions: cement [3]. Cement manufacturing is responsible for emitting more than 3 Gt/year of CO_2 globally (calculated from global cement production and CO_2/cement ratio in [4]) or about 8% of global CO_2 emissions. These emissions result from the calcination of limestone ($CaCO_3 \rightarrow CaO + CO_2$) and the combustion of fuels required to reach clinkering temperatures of 1450 °C. Key strategies to reduce the emissions include calcining less $CaCO_3$-containing minerals and combusting less fossil fuels for cement manufacture; therefore, alternative materials and radically new technologies are required. The vast availability of Fe-rich resources raises the question of whether these can provide part of the solution. Fe-rich materials which can be used economically for cement production and formulation are available worldwide, but they have not yet been fully exploited in the cement industry. Iron is usually known for not contributing much more than color and a lower processing temperature to cement clinker rather than for its cementitious properties. However, to enhance the alternative raw materials revolution and advance sustainable cement technology, incorporation of iron into cement products must be increased, accompanied with a reduced calcium content, and with iron contributing to the binding phases.

The variety of Fe-rich resources which can be alternative raw materials for cements can be divided in two large groups: natural resources and industrial by-products/residues. Natural resources that can be considered Fe-rich are certain types of clay and volcanic ashes. Depending on the location, these can be highly available and they are especially interesting in developing regions where industrial process residues are scarce or of poor environmental quality [4]. The range of Fe-rich industrial by-products and residues is very wide, resulting mostly – but not exclusively – from the production of metals. For example, the production of steel in the basic oxygen furnace or electric

* Corresponding author.
E-mail address: t.hanein@sheffield.ac.uk (T. Hanein).

https://doi.org/10.1016/j.cemconres.2022.106834
Received 22 December 2021; Received in revised form 4 May 2022; Accepted 6 May 2022
Available online 13 May 2022

arc furnace generates slag with a high content of FeO [5], while slags with a fayalitic composition (Fe_2SiO_4) originate from the pyrometallurgical processing of non-ferrous metals [5,6]. Although distinct from slags in most characteristics, hydrometallurgical process residues can also contain a high amount of iron [7,8]. The most abundant examples are bauxite residue, goethite residue, and jarosite sludges. Sludges from water treatment facilities can also have high contents of iron hydroxides [9].

Generalised discussion on the behaviour of iron in cement is difficult because of the wide variety in oxidation and coordination states in which the element can be found. The speciation and coordination of iron in the resource are key for its potential role in cements. If iron is present in a phase which is not soluble in the conditions of the chosen cement system, iron will not influence the reactions and will instead stay in the unreacted fraction of the hardened material. Therefore, detailed knowledge on the speciation of iron is crucial for determining the potential use of any resource in a cementitious material and its potential involvement in the reactions. On the other hand, the speciation of iron and therefore its role in cements can be altered by additional processes (e.g. calcination, vitrification). For crystalline materials a combination of determining the mineralogical phase composition using X-ray diffraction and determining the solubility of the iron-containing phases in aqueous environment will enable assessments of whether iron will influence the system. In case of (partially) amorphous materials the evaluation of the reactivity is more tedious as characterization of the structure needs more effort and a continuum of possible structures and reactivities exists [10]. An important example of an amorphous phase that can take part in cementitious reactions is a silicate glass, in which iron can be present in multiple oxidation states and coordination numbers [10].

Three main utilisation routes are identified to exploit the cementitious properties of Fe-rich resources:

(1) as raw materials for Portland or alternative clinker production
(2) as supplementary cementitious materials (SCMs) to partially substitute Portland cement, and
(3) as primary constituent of an alternative binder, most notably in alkali-activated materials (AAMs).

The raw materials used to produce Portland cement clinker already contain iron, which eventually generates the ferrite phase in the clinker [11]. A certain amount of iron is necessary in the raw meal to achieve the desired burnability, and Fe-rich material (e.g., limonite) is used in cement plants as a correctional raw material in the clinker raw meal when iron content is too low. Recent results indicate that ferrite-rich Portland cements can reach equivalent strengths to conventional Portland cement [12]. There is currently also a rising interest in the production of Fe-rich alternative clinkers such as ferritic calcium sulfoaluminate based cements or BYF (belite-ye'elimite-ferrite) cements, in which ferrite plays an important role in the main hydration reactions [13,14]. The use of Fe-rich SCMs delivers in many cases a satisfactory strength development and often only a slight change in reaction products is seen in comparison with traditional blended cements [15,16]. Fe-rich precursors for AAMs can, however, be associated with a larger change in reaction products relative to Portland cement [17,18], depending on the reactivity of the iron-containing phase, and iron speciation.

The aim of this review is to identify the Fe-rich materials available, and to present the state-of-the-art in the use of these materials for cements. Emerging technologies and opportunities are presented indicating priority future research directions. The role and extent of contribution of iron in clinkers, blended cements, and alkali activated materials is assessed. Special attention is given to the speciation of iron, as this influences how iron can participate in the cementation processes. The opportunities and challenges facing the use of Fe-rich materials are summarized, and the future of iron in cements is discussed.

2. Sources of Fe-rich materials available for use in cements

When focus is transferred from conventional (low-iron) calcium- and silicon-rich resources for cement production, to materials which can include a significant amount of iron, a pool of new resources is revealed. If a moderate content of calcium is still present, increased use of these materials in cement clinker manufacture will allow for the reduction in the use of the main calcareous source, limestone (mainly calcium carbonate), and will also enable improved process energy efficiency in the cement industry due to improved fluxing and lowered process temperature. In other cases, reactive silica, alumina, or iron in the resource may deliver a good quality SCM or precursor for AAMs. The resources available in relatively sufficient quantities are subdivided into natural resources and by-products/residues. The use of by-products and residues in cement will promote industrial symbiosis while enhancing resource efficiency and landfill diversion. Some of these Fe-containing "wastes" are hazardous and should not be disposed of in traditional ways; thus, converting them into cement products could provide the added benefits of immobilising the contaminants through cementation while also diminishing the cost of disposal. On the other hand, not all elements or concentrations can be sufficiently immobilized in a cementitious matrix to meet safety (e.g. leaching) standards, so in many cases it is more desirable to remove contaminants in part or in full, before introducing the decontaminated material into the construction material cycle [8].

2.1. Natural resources

2.1.1. Clays

The availability of clay resources matches well with the volumes of cement production at a global scale [4]. Clays are commonly used as a raw material for clinker production as a source of silica and alumina, and to a lesser extent of iron. In addition, by calcination at appropriate temperatures (650–950 °C), clays can be processed into a reactive material, suitable for use as SCM or AAM precursor. In the so-called LC^3 (limestone calcined clay cement), ~50% of Portland clinker is substituted by a combination of ground limestone and calcined clay [19]. Current research and production of calcined clays for use in cements mainly concerns kaolinite-rich clays, which can vary widely in iron content; additionally, because of their shared genesis as rock weathering products, kaolinite and iron (hydr)oxide minerals are often encountered together. Common clays, which contain mixtures of different clay minerals, normally contain up to several weight percent of iron (as Fe_2O_3), but lateritic soil can contain more than 40 wt% Fe_2O_3 [20]. Lateritic soil is rusty red due to the high presence of iron oxides and is formed by the long-lasting and intensive weathering of the parent rock. The global distribution of laterite and associated materials is broadly governed by world climatic zones [21,22]; laterite is normally found in tropical and subtropical zones. The clay mineralogical composition of this soil is frequently kaolinite occasionally sepiolite-palygorskite in e.g. Ni-rich laterites.

Lateritic soils are characterised by a higher proportion of iron and aluminium oxides compared to other soils. In ferruginous laterite soils, iron (hydr)oxide predominates, while alumina predominates in aluminous laterite soils. Iron in laterite – or clayey soils in general – is usually present as (hydr)oxide minerals, although a wide variety of minor minerals containing Fe^{2+} can also be present depending on the atmosphere and presence of anions, such as vivianite, siderite, and pyrite. In sulfur-rich and oxidising environments, jarosite is commonly formed. A common assumption – which requires further testing for confirmation – is that the reactivity of calcined clays as an SCM or a precursor for AAMs originates from the (meta)kaolinite phase in this type of clays and the involvement of iron is limited. Some involvement of iron is possible because of the small amount of aluminium substitution in kaolinite [23]. Substitution of iron in the kaolinite lattice has been correlated with higher degrees of structural disorder [24,25], and consequently lower clay calcination temperatures needed for activation (dehydroxylation)

[26]. As disordered kaolinites formed after calcination are noted to be more reactive than initially ordered kaolinites [27,28], iron substitution into kaolinite may also therefore increase the pozzolanic reactivity or the performance in AAMs [29]. In addition to the structural Fe, iron can also adsorb onto the clay surface from ground water but more research is required to understand if sorbed iron can contribute significantly in cementitious systems.

The potential use of clays in cements is not restricted to kaolinitic types; various iron-containing clays are ubiquitous in nature. Clay minerals from the smectite and illite group can have significant iron substitution in the structure and have shown to provide reactivity as SCM or precursor for AAMs [30–33]. The oxidation state and position of iron in the crystal structures of smectite and illite can be modified – including by (thermal) treatments or by natural processes – adding an important additional facet to understanding the structure and behaviour in cements of these Fe-rich smectites and illites [34,35]. Examples of clay mineral properties that are greatly affected by changes in iron oxidation state are swelling in water, cation exchange/fixation capacity, surface area, and surface pH. Dredging sediments often contain a combination of iron and clay minerals and therefore follow the same logic as clays; these are generated in Europe alone at 250–310 Mt each year (50–60 Mt freshwater, 200–250 Mt marine sediments) [36]. They have been mostly investigated after calcination as SCM [37–39] or as precursor for AAMs [40,41].

A non-exhaustive list of examples of Fe-rich clays and their chemical composition is provided in Table 1. A summary of cement binder precursors is also given in Table 1, which shows that clays can be incorporated in a range of cements. The clays described by Lassinantti Gualtieri et al. [42], Alujas et al. [43], and Kaze et al. [33] are lateritic clays with high Fe_2O_3 contents in the form of goethite and hematite. The behaviour of these clays as SCM or AAM precursor is usually determined by the kaolinite content, although a minor involvement of the Fe-containing phases in the hydration reactions is theorised in some works [29,33,44]. This is different for the smectite clays of Danner et al. [31] and Khalifa et al. [30], who showed that the smectite – containing iron – is the reactive part as SCM and AAM precursor, and iron will therefore play a role in the hydration of the cement or formation of the AAM binding phase.

2.1.2. Volcanic ashes

Volcanic ashes are estimated to cover 0.84% of the Earth's land surface [46], although obviously localized in regions of higher volcanic activity. The iron content can vary between 1 and 18 wt% Fe_2O_3, although most ashes contain around 10 wt% Fe_2O_3 [46]. The chemistry and mineralogy of volcanic ashes vary considerably depending on the eruption conditions and the type of magma from which they originate and their age or degree of weathering [47]. Most volcanic ashes are classified as natural pozzolans according to ASTM C618, if their sum of $SiO_2 + Al_2O_3 + Fe_2O_3$ is above 70 wt% [47–49]. In most cases SiO_2 is the dominant oxide, followed by Al_2O_3 and/or sometimes Fe_2O_3. The minerals found in volcanic ashes primarily originate from magma, but can also derive from the crust and upper mantle due to mechanical stripping during volcanic eruption. The minerals mainly include silicates, such as pyroxenes, amphiboles, micas, olivines, quartz and feldspar group minerals, Fe—Ti oxides, Ti-magnetite and ilmenite [48,50]. Volcanic ashes often contain a significant amorphous fraction. Iron can be present in the amorphous fraction or in pyroxenes, olivines, or oxides. In addition, exposure of volcanic ashes to weathering or diagenesis results in formation of secondary minerals such as clay minerals, zeolites, iron hydroxides, and carbonates [51].

Most studies on the reactivity of volcanic ashes as SCM are limited to the global assessment of the effect of the addition of the ashes on the physical properties of cements/concretes. The interplay between parameters such as the pozzolanic reactivity as SCM [52,53] and the ash fineness and the mineralogical composition have often been investigated. Reactivity as SCM tends to be associated with the amount of the amorphous fraction or zeolites [54], which usually react more rapidly in pozzolanic processes than the primary crystalline phases that react only slowly or not at all [48,49]. Depending on their properties, volcanic ashes can usually substitute up to 10–30 wt% of Portland cement in a blend without substantial alteration of the mechanical properties [48,49]. Beside their use as SCM materials, volcanic ashes are also suitable as precursors for AAMs, as evidenced by the substantial number of studies performed on their use as sole AAM precursor or in a blended AAM binder [48,55].

A list of example volcanic ashes and their relevant properties is shown in Table 2. The quality of volcanic ashes as SCM or in AAMs seems to result mainly from the reactivity of the amorphous phase [56–58], or occasionally from the presence of zeolite or clay phases [59].

2.2. By-products and residues

The use of by-products and residues improves the sustainability of a cement from a resource efficiency point of view, through waste valorisation. On the other hand, this makes the supply (and quality) of the material dependent on the production process of the main product

Table 1
Chemical compositions and main minerals in the example clays and a summary of the observed behaviour for the studied binder type. Chemical/oxide compositions were taken from the cited papers (before calcination if calcination was carried out in in the reference).

Reference	wt% Fe_2O_3	wt% SiO_2	wt% Al_2O_3	wt% CaO	Minor elements > 1 wt%	Main minerals > 5 wt %	Major iron-containing mineral	Cement type	Observations
Alujas et al. [43]	11.1	43.8	24.7	1.4	Mg, K, Na	Kaolinite, montmorillonite. Illite	Hematite	SCM	High contribution to strength development; reactivity mainly from kaolinite
Danner et al. [31]	10.4	48.7	17.8	13.8	Mg, K	Smectite, calcite	Smectite	SCM	Good mechanical properties; dissolution of iron compound
Irassar et al. [45]	7.8	60.3	17.9	0.6	Mg, K	Illite, quartz	Chlorite	SCM	Low reactivity after calcination
Kaze et al. [33]	41.0 44.3	25.6 22.3	17.9 14.9	0.1 1.0	Ti Ti, K	Kaolinite, quartz, hematite/goethite	Hematite, goethite	AAM	Decent mechanical properties; dissolution of iron; limited involvement of iron in AAMs
Khalifa et al. [30]	17.5	43.4	10.7	1.9	Mg, Ti	Illite, smectite	Smectite (nontronite)	AAM	Low/moderate reactivity after calcination
Lassinantti Gualtieri et al. [42]	20.4	43.8	24.8	0.1	Mg, Ti	Kaolinite, quartz	Goethite, hematite	AAM	Calcination required for activation; AAM probably only from reaction of metakaolin
Snellings et al. [37]	9	37	10	12	Mg, K	Illite, quartz, calcite	Fe-hydroxides, pyrite	SCM	Moderate reactivity after calcination; pyrite converted to iron oxides and anhydrite by calcination

Table 2
Chemical compositions and main minerals in the example volcanic ashes and a summary of the observed behaviour for the studied binder type. Chemical compositions are taken from the cited papers.

Reference	wt% Fe_2O_3	wt% SiO_2	wt% Al_2O_3	wt% CaO	Minor elements >1 wt%	Main minerals >5 wt%	Major iron-containing phases	Cement type	Observations
Al-Fadala et al. [53]	13.3 12.2	46.5 44.5	13.5 13.5	9.4 9.3	Mg, Ti, K, Na	Anorthite, albite, forsterite	Forsterite	SCM	No/minor contribution to strength development (coarse ashes)
Bondar et al. [59]	1–4	61–70	11–16	2–8	Mg, K, Na	Albite, quartz, hornblende, montmorillonite, biotite	/	AAM	Calcination of ashes increases strength of AAMs in some cases
Celik et al. [57]	12.2	46.5	14.7	8.8	Mg, Ti, K, Na	Anorthite, diopside, forsterite, amorphous palagonite-like glass	Amorphous	SCM	Good quality self-compacting concrete with 55 wt% cement replacement; significant reaction of the amorphous phase; resistance to chloride migration increases with ash addition
Hossain [60]	7.1	59.3	17.5	6.1	Mg, Na, K	/	/	SCM	Minor contribution to strength development; minor effect on alkali-silica reaction
Lemougna et al. [58]	8–14	43–55	15–16	6–11	Mg, Ti, K, Na	Anorthite, forsterite, quartz, augite	Forsterite, augite, hematite, magnetite	AAM	More amorphous fraction gives higher reactivity; good compressive strength in blocks
Zhou et al. [56]	12–17	43–44	16.6	8.1	Mg, Ti, K, Na, P	Diopside, albite, amorphous	Forsterite, amorphous	AAM	NaOH-activated material strength is very dependent on ash sample

generating waste, although the security of supply for the cement industry can be assured through long-term contracts. The list of Fe-rich by-products and residues in Table 3 is focused on streams with a significant volume from a global perspective. The side streams are summarized in Table 3, showing a wide range of iron contents. The major phases in each stream are indicated. The industry of origin and an estimate of the global production are provided. A more detailed discussion of these aspects, including the calculation carried out to obtain the global production figures and block-flow diagrams of the process of origin, is given in the respective subsections (Sections 2.2.1–2.2.5).

2.2.1. Steel slags

The most common route to produce primary steel is through the smelting of iron ore in the blast furnace to produce pig iron (and blast furnace slag as a by-product), followed by steelmaking in a basic oxygen furnace (BOF) [5], see Fig. 1. The recycling of steel (secondary steel making) is carried out in an electric arc furnace (EAF), which is also the type of furnace used to produce stainless steel. The slags resulting from the BOF and the EAF are to some extent similar in composition and therefore discussed together in this section [72]. Ladle slags are another type of by-product that is generated in the steel production flowsheet. Despite being researched for use in alternative binder systems, ladle slags are not generally so rich in iron and are therefore not within the scope of this review paper [73]. Global steel production accounted for 1.9 Gt in 2020, of which 71% was produced using the blast furnace – BOF (primary route) and 29% was produced in the EAF (by recycling of scrap) [74]. The annual production of stainless steel is much lower, being estimated at 50.9 Mt [75]. The metal/slag ratio in (non-stainless) steel production is similar in both furnace types, and slag volumes can be estimated at ~14 wt% of the steel production [64]. In stainless steel production the metal/slag ratio is lower and estimations are closer to a 3/1 ratio. Global steel slag production can thus be estimated at 1878 × 0.14 Mt (steel) + 50.9 × 0.33 Mt (stainless steel) = 280 Mt.

Nearly half of steel slag is composed of CaO, making it a useful de-

Table 3
A list of major side streams containing high percentage of Fe with potential for beneficial use in the cement industry. Materials which would normally undergo a further economic metal extraction step are not included.

Side stream	Fe_2O_3[a] wt%	Other major (>3%) constituents (represented as oxides)	Major phases (>5 wt%)	Potentially toxic elements of main concern	Source	Generation p. a. (Mt)
Steel slags (basic oxygen furnace & electric arc furnace slags)	13–27 (1–50) [61,62]	CaO, Al_2O_3, SiO_2, MgO	Belite, alite, lime, wustite, ferrite, merwinite, periclase	Cr, V [5]	Steel and stainless steel production	280 [62–65]
Bauxite residue	25–60 (5–60)[b] [66]	Al_2O_3, SiO_2, Na_2O, CaO, TiO_2	Hematite, goethite, Al-hydroxides, de-silication product[c], Ti-oxides, calcite, perovskite/ilmenite	Cr, As, V, (Co, Mo, Ni) [67]	Primary alumina production	180 [66]
Fayalitic non-ferrous metallurgy slag	40–60 [5]	SiO_2, CaO, Al_2O_3	Amorphous glass, fayalite, spinel	Pb, Zn, (Ba, Cu) [5]	Non-ferrous metal production (Cu, Ni, Sn, Pb)	58 [5]
Zinc production sludges (goethite & jarosite residues)	23–45 [8,68]	SO_3, ZnO, PbO, Na_2O, SiO_2	Jarosite, goethite, sulfur, iron/zinc sulfide, gypsum, quartz	Pb, Zn, As, Cd [8]	Primary zinc production	6 [8,69,70]
Ferric water sludge	15–58 [9]	CaO, SiO_2, P_2O_5, SO_3, Al_2O_3	Ferrihydrite, amorphous iron oxide	Zn, Pb, Cd, Ni, Cu, Cr, Co [9]	Water treatment	3

[a] Although Fe is presented as Fe_2O_3, the iron may exist in other oxidation states (FeO, Fe). Chemical compositions on dry basis without normalization are used to report the Fe_2O_3 content. A representative range for most residues of the type is provided, sometimes complemented with a range between brackets representing all compositions that can be found in literature.

[b] Most bauxite residues originate from the Bayer process with Fe_2O_3 contents of 25–60 wt%. Some plants, mostly in China, use a sintering process before the hydrometallurgical process. These plants can treat other ores which usually have a higher SiO_2 content and lower Fe_2O_3 content, hence the range shown of 5–60 wt%.

[c] De-silication product is a common term for phases resulting from the reaction of the Bayer liquor with silicates from the bauxite ore. Most commonly, sodalite or cancrinite are present.

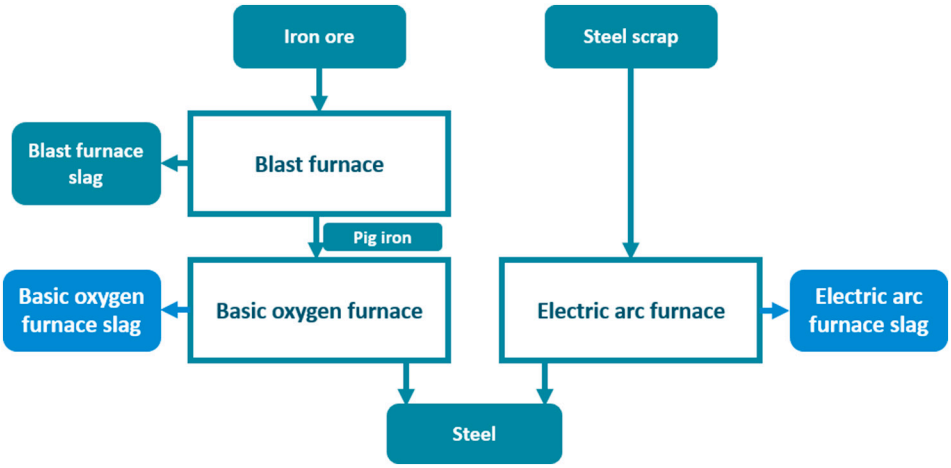

Fig. 1. Block-flow diagram of primary and secondary steel slag production.

carbonised Ca source for cements [65,76]. It is therefore currently already used as a calcium/iron correctional source in the production of conventional Portland cement clinker in some countries (e.g Belgium) [77], and can also be used in high percentages for the synthesis of ferritic calcium sulfoaluminate-belite cements [13,78,79]. Steel slags often contain around 20 wt% Fe oxides, with a variable oxidation state. The iron is distributed between ferrite and wüstite-like (denoted "RO" for divalent metal oxide) solid solution phases. Other hydraulic phases such as belite, alite, and (free-)lime or periclase are commonly found in steel slags. Despite the presence of a high amount of calcium and hydraulic phases, the reactivity of steel slags as SCM is rather low and the contribution to strength is limited [80–82]; substitution rates up to 20 wt% in blends with Portland cement provide satisfactory performance [80,83]. As a precursor for AAMs, steel slags have shown promising results in terms of strength evolution [84]. The granular form and high hardness of most steel slags leads to their use as aggregates in road base or asphalt, which is currently the main application for these materials. However, there may be issues of expansion and soundness associated with the presence of high free lime content, as well as in terms of heavy metal leaching on which legislation has tightened in several countries.

2.2.2. *Bauxite residue*

Alumina is produced in the Bayer process, which extracts sodium aluminate from bauxite ore [66,85] (Fig. 2). The solid residue from this process is called bauxite residue, sometimes referred to by the more popularised name "red mud". The world average refinery produces about 1.35 t of bauxite residue for 1 t of alumina [66]. The production of alumina in 2020 was approximately 134 Mt resulting in the generation of over 180 Mt of red mud [86]. The current utilisation rate of bauxite residue is around 3%; most is landfilled or stored in ponds [66,85], and the worldwide inventory is now over 3 Gt [85,87]. Bauxite residue is considered a hazardous material and known for its major disposal problems which includes high alkalinity [88]. The large amounts produced are also a serious threat through potential landslides or dam collapses, as took place in Hungary in 2010.

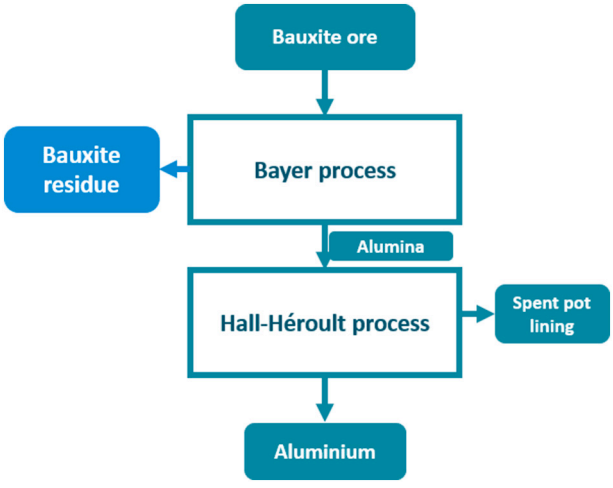

Fig. 2. Block-flow diagram of primary aluminium and bauxite residue production.

Iron is the major element in bauxite residue, present in the form of hematite and goethite. Most bauxite residues have 40–50 wt% Fe_2O_3, although some fall in a wider range of 25–60 wt% Fe_2O_3. Second in abundance are usually Al_2O_3 (~20 wt%) and SiO_2 (10–15 wt%). Significant amounts of sodium, calcium and titanium are present (0–8 wt %). The low calcium content makes the bauxite residue a less obvious choice for the production of clinkers. Despite that, the 3% of bauxite residue which has a useful application is mostly applied as a correctional iron source in the production of Portland clinker [66,85] and bauxite residue has been investigated to be used in high volumes (>30 wt%) in the production of calcium sulfoaluminate cement [14]. The use of bauxite residue as SCM has not shown consistently positive results. The pozzolanic reactivity of untreated bauxite residue is low and the presence of soluble sodium negatively affects workability while accelerating the setting and hardening of the cement [89–94]. In other words, only low cement clinker replacement levels (~10 wt% cement substitution) are recommended when using bauxite residue as is. An improvement of the behaviour as SCM can be accomplished by high-temperature treatments. A calcination process at 800 °C in the presence of kaolinite showed an improved reactivity and decreased the soluble sodium [89], while a melting and quenching process transformed the bauxite residue into a slag [95]. The use of these modified bauxite residue slags in alkali-activated materials has been studied successfully as well [96–98].

The use of non-treated bauxite residue in alkali-activated materials has also been widely investigated with varying results, i.e. good properties can be obtained in specific cases. A review paper on this specific topic was written by Hertel and Pontikes [99]. As well as using the solid part of the bauxite residue slurry, alkali-activated materials can also incorporate the alkaline liquid part of the slurry [99].

2.2.3. *Fayalitic non-ferrous metallurgy slags*

The family of fayalitic slags has their chemical composition as a common characteristic, being close to the mineral fayalite (Fe_2SiO_4). These slags originate from the primary and secondary production of non-ferrous metals, such as copper, nickel, lead, and tin (see block-flow diagrams in Fig. 3). Primary copper production is the largest source of

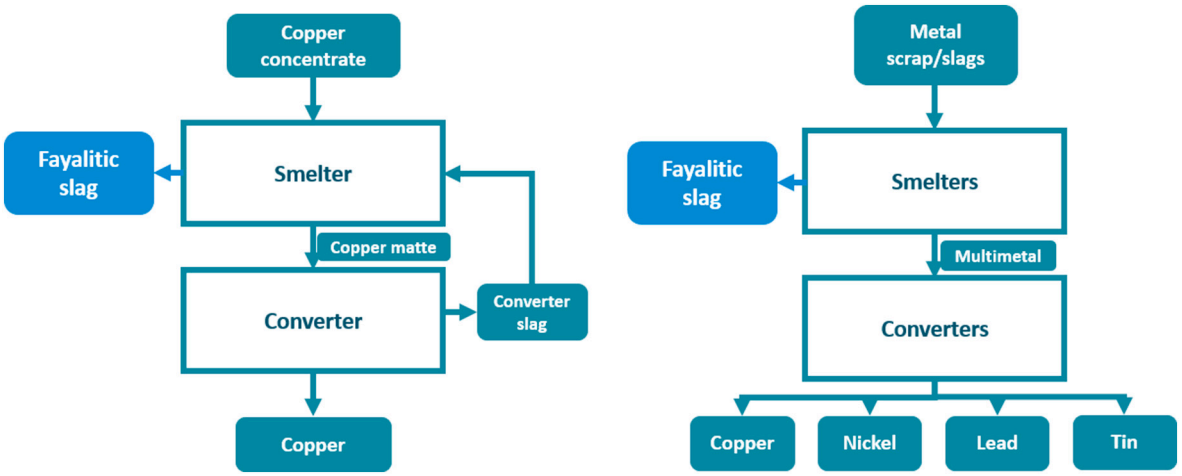

Fig. 3. Block-flow diagram of primary copper and secondary non-ferrous metal production resulting in fayalitic slags.

fayalitic slags. 20 Mt of copper is mined yearly [100,101] and for each tonne of primary copper 2.2 t of fayalitic slag is produced [6], resulting in a global total of 44 Mt of fayalitic slag from primary copper production. Approximately 30–35% of the copper supply is produced by recycling of scrap according to most sources [102]. The total production of copper is 24 Mt [103]; this difference from the result of a simple summation of mined and recycled copper (30 Mt) originates from the fact that most copper scrap is incorporated in the primary copper production chain, leaving only 4 Mt of purely secondary produced copper [104]. Assuming a similar ratio of metal/slag, this 4 Mt of recycled copper would result in 8.8 Mt of additional fayalitic slag. Furthermore, the secondary production of copper often goes together with other non-ferrous metals, such as lead, nickel, and tin. As such, the 8.8 Mt of fayalitic slag is probably a good estimation for the complete global secondary fayalitic non-ferrous metal slag production. To the above estimated amounts, slags from primary nickel and tin production must be added. Primary nickel production is estimated at 2–3 Mt [105,106] and primary tin at 0.3 Mt [107]. Residues from primary nickel production are variable, due to a variation in the production processes that are used. However, fayalitic slags are significantly produced in the primary nickel flowsheet [13]. In summary, this assessment shows that a calculation of the global production of fayalitic non-ferrous metallurgy slag is cumbersome, but will be in the range of 58 ± 8 Mt/y.

Apart from the major elements iron and silicon, significant amounts (0–8 wt%) of calcium and aluminium are present in fayalitic slags. The phase composition is influenced by the cooling conditions after the pyrometallurgical process. Fayalitic slags are often quenched – similar to blast furnace slags – to obtain a significant fraction of amorphous phase. Depending on the specific composition and the quenching technology 40–100% of amorphous phase can be obtained. When the slag is cooled slowly, the fayalite mineral is the dominant phase. Minor phases are often spinels or iron-oxides. Fayalitic slags might be used in the raw meal for the production of Portland clinker as iron and silica source to improve burnability or lower the clinkering temperature. However, only a small proportion of the clinker raw meal can currently be replaced in Portland cement manufacturing. A higher percentage can be used in the synthesis of a calcium sulfoaluminate cement, in which a fayalite slag content of 17 wt% resulted in a similar strength as a reference cement mixture [13]. Another application of fayalitic slags in cements with successful results in literature is the use of quenched slags as SCM or as precursor for AAMs. In terms of reactivity as SCM, the quenched fayalitic slags reach values similar to class F coal fly ashes [15,108,109]. Also AAMs can be produced from fayalitic slags with equivalent performance to common Portland cement blends [110–113]. The nanostructure of these AAMs is completely different in comparison with conventional fly ash and blast furnace slag-based AAMs, due to the significant participation of iron in the reactions and the role of iron in the structure [17,114]. This will be elaborated in Section 4.3.

2.2.4. Zinc production sludges

Zinc is produced globally mainly through a hydrometallurgical process route, schematically shown in Fig. 4, where zinc sulfide concentrates are treated through the Roast-Leach-Electrowinning process [115]. The leaching process delivers, next to a zinc-rich leachate, also an Fe-rich solid residue as a sludge. Three main leaching processes exist, which are named by the dominant mineral in the solid residue they generate: the jarosite process, the goethite process, and the hematite process (the latter is not widely used) [115]. Globally, the main production route is the jarosite process [116], producing 0.5 t of jarosite residue per tonne of zinc. In Europe a significant amount of plants apply the goethite process for the extraction of zinc [8]. Goethite residue results from this process in a ratio of 0.33 t/t Zn. Global zinc production is estimated at 13 Mt [70,117] and an estimate of the total production of jarosite and goethite sludges of 6 Mt can thus be derived from the zinc volume and sludge/zinc ratios.

The iron content of zinc sludges falls in a range of 23–45 wt% Fe_2O_3 [8,68]. The major phases in jarosite and goethite sludges are, by definition, jarosite and goethite respectively. Jarosite and goethite waste both contain high concentrations of potentially toxic elements, such as residual heavy metals (e.g. Pb, Zn, Cd, As) and non-metal components (high sulfate or elemental sulfur content in jarosite), and these sludges are therefore universally categorized as hazardous waste. Furthermore, the metal content is often sufficiently high to stimulate research into

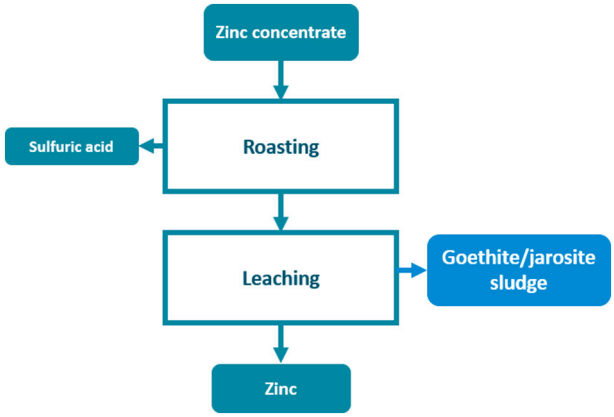

Fig. 4. Block-flow diagram of primary zinc and goethite/jarosite sludge production.

metal recovery processes. Most literature therefore applies an additional treatment before the use of the sludge in cement. A pyrometallurgical fuming process can volatilise the heavy metals and deliver a clean slag [118], which can be used as SCM or in AAMs [119]. Hydrometallurgical and solvometallurgical processes also exist to extract metals from jarosite or goethite residue [8,120,121]; however, their valorisation as SCM or in AAMs might be less straightforward due to the mineralogy of the resulting solid residue, which will mostly be composed of jarosite and goethite and therefore less reactive in the cement formulation (Section 3). This is not an issue for application in clinker manufacturing.

2.2.5. Ferric water treatment sludge

Clean drinking/potable water is a vital resource that involves an established treatment process to remove contaminants [9,71]. Potable water treatment, shown schematically in Fig. 5, involves dosing a coagulant, which then forms precipitates in the water. The most used coagulants are aluminium sulfate (alum) and hydrolysing trivalent iron salts such as ferric sulfate or ferric chloride; a combination of these can also be used. The precipitates cluster with the contaminants in the raw water and are held together suspended in the purified water; the solid can be formed into larger flakes by addition of a flocculant. The supernatant stream is then taken off for possible further processing and distribution to customers. The separation of suspended solids is normally carried out by gravity settling (sedimentation or clarification), and/or filtration or flotation. The sludge by-product is discharged into sewers or pressed into cake and landfilled. Sludge production is increasing due to higher levels of treatment and greater volumes of clean water needed globally. A conservative estimation of the global volume can be derived from the production of 1 t (dry matter) per 1000 people [71], resulting in a total generation of 8 Mt p.a. Fe-rich water treatment sludges account for about 1/3 of the total, so a rough estimation of the global Fe-rich water treatment sludge production is 2.7 Mt/year.

Sludge formed as a result of coagulation of backwash water from filters removing (or oxidation of) iron and manganese from groundwater are also Fe-rich and can have potential re-use in cements [122]; they are usually classified as non-problematic. Other problematic sludge wastes can also arise from the treatment of various types of contaminated waters, whereby hydrous metal oxides are used to adsorb hydrolysable contaminants from solution, such as heavy metals – particularly arsenic – or radionuclides [123,124]. In many cases, ferric oxides are used [125,126].

The iron-containing component of the sludge is initially made up of a disordered ferrihydrite phase ("2-line ferrihydrite"), but may become more crystalline overtime and transform into hematite, goethite or other iron (oxy)hydroxide phases as it ages [122]. Given that the sludges contain a high water content (up to ~90%), the iron phases are almost always hydrous or hydroxide-containing. The remaining content of the sludge waste can vary, depending on the particular treatment method used, but can include salts and organics derived from the different flocculation methods adopted. There have been studies considering cements containing ferric sludge wastes [127–129]. The replacement of Portland cement by up to ~2 wt% sludge retarded hydration to a certain extent, but the compressive strength (after 28 days) was not significantly reduced [127]. However, when additions of sludge wastes exceeded ~2 wt%, heat evolution and extent of reaction was significantly reduced. Compressive strength of the final hardened composite was also drastically decreased with sludge additions beyond 2 wt% [127,128]. CSA cements were blended with technologically desirable properties including up to 35 wt% of sludge as SCM [129]. Whilst Gomes et al. [127] generally considered that ferric sludge additions did not contribute to the formation of alternative Fe-bearing hydration products, or in fact, allow any significant incorporation of Fe into pre-existing binder phases [127], this is disputed by other studies. Using Fe K-edge X-ray absorption spectroscopy, the speciation of iron was observed to change from a hydrous ferric oxide coordination environment within the sludge, to that of a siliceous hydrogarnet phase within the Portland cement mixes [128]. The formation of an iron-substituted hydrogarnet phase was confirmed, while also the possibility of have iron substitution in the C-S-H phase was suggested if the sludges were pre-treated with slaked lime before blending with the cement [130,131].

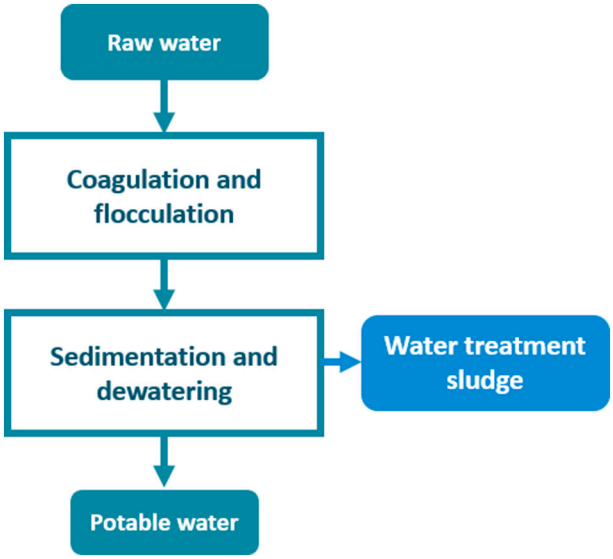

Fig. 5. Block-flow diagram of a water treatment process.

2.2.6. Comments on occupational exposure risks and environmental compatibility

By-products and residues tend to contain elevated concentrations of potentially harmful compounds. For most raw materials discussed in this section, the problems are mostly related to compounds of inorganic nature such as heavy metals or metalloids. These compounds may be released to the environment and cause harm to human health and ecosystems. Less frequently, the occupational or environmental hazard stems from radioactivity (e.g. in certain industrial effluents), organic compounds, pH, or release of anions (e.g. Cl^-, SO_4^{2-}). In most countries or regions that implemented waste management policies, the recycling of residues into new products is subject to strict regulation to contain exposure risks to users or the environment. Usually a first step is the comparison of total concentrations of potentially harmful compounds against limit values laid down by national or regional legislation. If certain total concentrations exceed limit values, the residue is either ruled out for any recycling, or compliance to emission limit values needs to be demonstrated to gain permission for recycling (to reach an End-of-Waste status). The specific scenario depends on the type of potentially harmful compound (e.g. organic vs. inorganic), the region or country, and the intended use.

For construction applications of Fe-rich residues usually a leaching test is imposed to verify environmental compatibility of the developed binders [132]. Several approaches to measuring leaching are practised [133]. Service life compliance of cement-bound material is often measured on monolith specimens of specified size that are immersed in a leaching solution enabling the contaminants to dissolve and diffuse from the specimen (e.g. EN 16637-2:2021). Such dynamic surface leaching tests on monoliths are typically time-consuming and do not cover the end-of-life or second life stages in which the material is crushed and recycled, for instance as unbound road base. More intense leaching tests on broken rubble of specified granulometry are therefore often prescribed. Examples are shaking tests of broken material in an aqueous leaching solution (e.g. EN 12457-4:2002) or upflow column percolation tests of leaching solution through a packed bed of crushed material (e.g. EN 16637-3:2021).

The containment of potentially harmful compounds by cement-stabilization of industrial residues is common practice in waste

management of effluents, chemical, metallurgical, incineration, and even nuclear waste [134–138]. Solidification by binders can be an effective means to immobilise and contain the release of harmful substances. The main chemical mechanisms that control the release of metals and metalloids are: i) the pH dependence of the solubility of the mineral compound that contains the element of concern, ii) the speciation of the element of concern which can change by reaction with the cement, and iii) adsorption of the element of concern on co-occurring phases [139]. For a given element of concern the dominant immobilisation mechanism can differ by cement type. For instance, the immobilisation of oxyanions such as chromate or arsenate by incorporation into ettringite is a well-known immobilisation mechanism in Portland cements [140] or calcium sulfoaluminate cements [141]. Minor levels of metals such as Zn, Cu and Pb can be incorporated into or sorbed onto Portland cement hydration products such as C-S-H [142–144].

Hydrated Portland cements where copper slag was used in the raw meal of the clinker showed limited mobility of the Ba, Cr and Cu [145] or Zn, Ti, Cu and Mo [146] that was present in the slag. The leaching of Pb is increased by the addition of the copper slag [146]. The addition of bauxite residue to the Portland clinker raw meal can increase the soluble Cr in the cement [147]. In alkali activated materials, the leaching of cationic species such as Pb and Zn is less problematic than anionic species such as As and V, because cationic species could be more easily chemically bound within the cementitious phases [148,149]. In contrast, elements such as As and V would be oxyanionic under highly alkaline conditions and consequently not able to neutralize the negative charge of Al in AAMs, for example, or to be precipitated as hydroxides. These elements may not be well bound in the cementitious binder if there are no sorption or incorporation sites for the negatively charged species, that therefore remain loosely bound and may leach out easily. In general verification of environmental compliance is an absolute requirement in the development of binders incorporating Fe-rich residues. In many cases it can be the most challenging target to meet, in particular when using residues with elevated total concentrations of elements of concern. Leaching compliance testing should therefore be taken along as early as possible in research and development programs.

2.2.7. *Limitations of this review regarding by-products and residues*

2.2.7.1. Mine tailings. The global annual production of mine tailings is estimated at 7 Gt [150], significantly surpassing all residues in Table 3. Most tailings contain iron and some sulfidic tailings have pyrite (FeS_x) as the major phase. However, the chemical and mineralogical variability of tailings is so high that a separate dedicated review paper would be necessary to cover all necessary nuances with respect to their behaviour in cements. Examples of such review papers are written by Gou et al. [151] and Martins et al. [152].

2.2.7.2. Other residues. Other residues have not been included in the discussion in this section to allow focus on the most abundant and richest in iron. Examples of such streams are municipal solid waste incineration ash or construction and demolition waste. Although abundant, the concentration of iron in these streams is rather low in comparison with the rest of Section 2.2. The iron in these raw materials would thus not influence the phase assemblage after clinkering as much as the raw materials in Table 3 or iron would not participate significantly in the reactions as SCM or AAM. Other process residues with relatively high iron content are also known, such as non-fayalitic non-ferrous metallurgy slags, but the volumes are rather low in comparison with the resources in Table 3.

3. The importance of speciation of iron for the use in cements

The production of Portland or alternative clinkers involves a high temperature process, which completely transforms the mineralogy of the raw materials. It therefore also transforms the iron-containing phases and changes the participation of iron in the cement hydration processes; this is not the case for the direct use as SCM or in AAMs. For assessing the role of iron in an SCM or precursor for AAMs, the distribution and speciation of Fe in the resource is crucial to avoid pre-processing. Iron will not influence the reactions if it is present in a phase which does not dissolve at the conditions imposed by the cement type, i.e. the phase in which iron is present has to be soluble at alkaline conditions. More specifically, the iron is preferably in a clay phase, the ferrite phase, a silicate glass, or another reactive Fe-containing phase to extensively partake in the formation of the binding phases as SCM or AAM precursor. Iron-oxides and goethite are usually stable at high pH and will thus remain as inert filler in the blend, although there is a non-negligible reactivity and involvement of amorphous iron hydroxides as SCM or AAM, which was shown by the change in speciation of iron from waste water treatment sludge when used as SCM [130,131]. Similar to crystalline iron oxides and hydroxides, crystalline iron-silicates – such as fayalite – have a limited solubility in conditions relevant for SCMs and AAMs [110,153] and will mainly have an influence as filler on the formation of the cement binder. Also, the small amount of Fe in blast furnace slags, present largely in metallic form, does not have an impact on the reaction products or reactivity of the slag [154,155]. Furthermore, the oxidation state of iron in the precursor and the resultant cement pore solution is important for determining the role of iron in the hydrate phase assemblage [156], which will be discussed in more detail in Section 4.

Given the importance of speciation, it becomes clear that not all of the resources discussed in Section 2 present a precursor for which iron be available for reaction as SCM or in AAMs, if no treatments on the resource are carried out before utilisation. In lateritic clays, bauxite residue, and zinc sludges, the iron is mostly present as hematite or goethite. Smectite clays can have a significant amount of iron in the clay minerals, which become reactive after calcination.

Mössbauer spectroscopy was used to investigate the influence of iron speciation in two volcanic ashes on their alkali-activation [157]. In the ashes, the iron was present in the pyroxene augite ($CaMg_{0.74}Fe_{0.25}$) Si_2O_6, the olivine forsterite, $(Mg_{0.9}\ Fe_{0.1})_2SiO_4$ and in the amorphous fraction. These three species of iron reacted differently: the forsterite in the original ashes remained unaltered, while a substantial fraction of augite dissolved and reacted, causing the iron to be incorporated in the binding phases of the alkali-activated material [157].

The behaviour of steel slags can be engineered, as the interaction between the chemical composition and cooling conditions will determine the phase composition and whether a reactive phase is present with iron inside [84,158,159]. For fayalitic slags, the importance of quenching is underlined further. A large fraction of iron silicate glass can be obtained after quenching, delivering significant reactivity in alkaline environments. If the slag is cooled more slowly, the reactivity drastically decreases, as crystalline iron silicates form more readily and are much less reactive [153,160]. Iron silicate glasses show a continuum of possible structures and resulting reactivities. The coordination number and oxidation state of iron can be varied, but most of all, the presence of other elements such as calcium and aluminium, and the Fe/Si ratio, have a large influence on the reactivity of the glass [114,161,162].

It remains to be seen whether it is important to maximise iron participation in the reactions towards a binder material: The precipitation of Fe-rich crystalline phases during pre-processing also changes the chemical composition of the glass, which might make the residual glass phase more reactive [163]. In other cases, for slags with a fayalitic composition, maximisation of the amorphous phase (and thus also the iron in the amorphous phase) increases the reactivity [153,160]. The resources in Section 2 can also be treated to increase the reactivity or decrease the release of potentially toxic elements. Such a treatment can result in a change in the speciation of iron. Hydrometallurgical treatments are important for the extraction of residual metals, but have a limited influence on the coordination environment of iron.

Pyrometallurgical treatments do completely change the phase composition and speciation of iron. For example, a fuming process has been developed for the extraction of zinc and lead from goethite residue, leaving an iron silicate slag, similar to fayalitic non-ferrous slags [119]. The transformation of bauxite residue into a slag specifically targets an increased reactivity as precursor for AAMs or as SCM [96].

4. Fe-rich cement types

The main uses of Fe-rich raw materials in cements can be divided into three types: Fe-rich cement clinkers, Fe-rich supplementary cementitious materials, and Fe-rich alkali-activated materials. One subsection here is dedicated to each of the three types. Each subsection starts with a general explanation of the material system, after which the effect of introducing a high amount of iron is discussed, regarding 1) the technical performance and 2) the hydrate assemblage or structure of the binding phases. Most of the discussion is not specific to particular raw materials among those described in Section 2, but rather this discussion aims to paint a generic picture taking into account the speciation requirements from Section 3.

4.1. Fe-rich cement clinkers

Clinker is the main reactive component of a traditional cement. For the technical performance of clinkers, the origin of the resource does not play a role. The starting phase composition and the speciation of iron do not influence the phase composition at temperatures relevant for clinkering; only the total chemical composition of the raw materials and specific conditions of the high temperature process and cooling regime determine the final phase composition and the quality of the clinker. Therefore, if a process works for one of the resources in Section 2, it will work the same for another resource if the mass balance of all elements is kept constant. In other words, Section 3 of this paper is not relevant to clinkers. The ASTM C150-21 standard has maximum limit values for the amount of iron in type II ($Fe_2O_3 \leq 6.0$ wt%) and type IV ($Fe_2O_3 \leq 6.5$ wt %) clinkers, but such limiting values are not present in EN standards. Iron in cement clinker is mostly found as calcium aluminoferrite whose (thermo)chemistry is next discussed (Section 4.1.1). The discussion of iron in clinkers is relevant to Portland cement clinker (Section 4.1.1), calcium sulfoaluminate(-ferrite) cement clinker (Section 4.1.2), and calcium aluminate(-ferrite) cement clinker (Section 4.1.3). A visual summary of this section is provided in Fig. 6.

4.1.1. Calcium (alumino)ferrite: chemistry and thermodynamics

The calcium aluminoferrite phase in cement clinker, ferrite, is normally one or more solid solutions in the series C_2F – C_6A_2F. The Bogue equations predict that every gram of Fe_2O_3 will result in approximately 3 g of ferrite [164], based on the assumption of formation of stoichiometric C_4AF. Typical ferrite minerals in present PC and CSA clinkers are brownmillerite (C_4AF) and srebrodolskite (C_2F); these minerals represent the end-members of a continuous solid solution defined by the value of x in the formula $Ca_2(Fe_{1-x}Al_x)_2O_5$, where $0.0 \leq x \leq 0.7$ [165]. The position in the brownmillerite-srebrodolskite solid solution varies in different clinkers, and for simplicity is usually called ferrite. The ferrite phase can have different variations depending on the Al and Fe levels, for example C_2F, C_6AF_2 and C_4AF [12,166,167]. The iron/aluminium (F/A) ratio is an important factor to control the ratio between ferrite and tricalcium aluminate [11]. The literature on the production of pure or a solid solution of ferrite phases is scarce, and the reproducibility of some studies is questionable [168], which is mostly attributed to the difficulties of characterising these phases; however, a recent study [169] has shown that firing at a temperature of 1350 °C was sufficient to produce pure C_4AF in a monophase system.

Thermodynamic simulations can be used to understand the equilibrium phase assemblage during clinkering; thermodynamics has been identified as an important tool in optimising clinker and developing novel clinker [170]. Thermodynamic data for the ferrite system do exist [171] and although not developed for clinker, can be used to a certain extent to understand experimental observations. Fig. 7 shows an isopleth in the C-F-A ternary diagram where $p(O_2)$ is set a 0.21 atm and x (CaO) is set at 0.6667; i.e., $C_2(A,F)$. The first black vertical line at x (Fe_2O_3) = 0.1666 represents C_4AF while the second vertical line at x (Fe_2O_3) = 0.25 depicts a high F/A ratio of $C_4A_{0.5}F_{1.5}$. The diagram indicates that upon cooling, various ferrites and/or aluminates can crystallise. Indeed, this has been confirmed through laboratory experiments (data not shown here) and confirms the importance of cooling in ferrite.

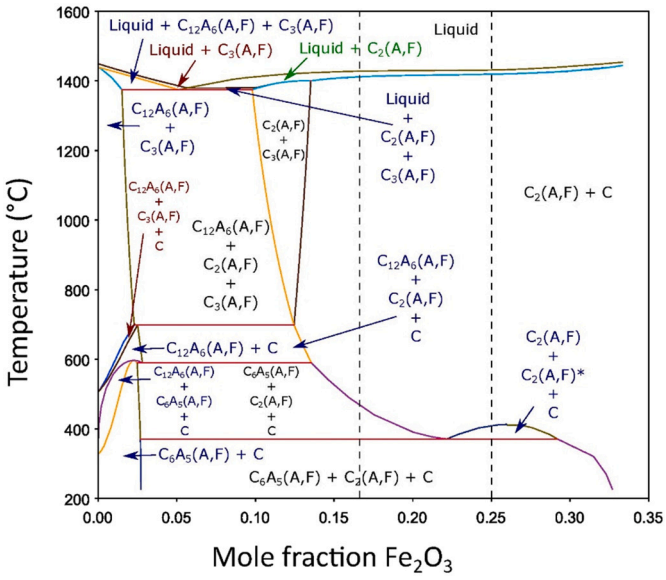

Fig. 7. Isopleth in the CaO-Fe_2O_3-Al_2O_3 ternary diagram in air ($p(O_2)$ = 0.21 atm) where x(CaO) = 0.6667 showing ferrite $C_2(A,F)$ stability calculated using Thermo-Calc 2020b software and OXDEMO: Oxide demo database v2.0.

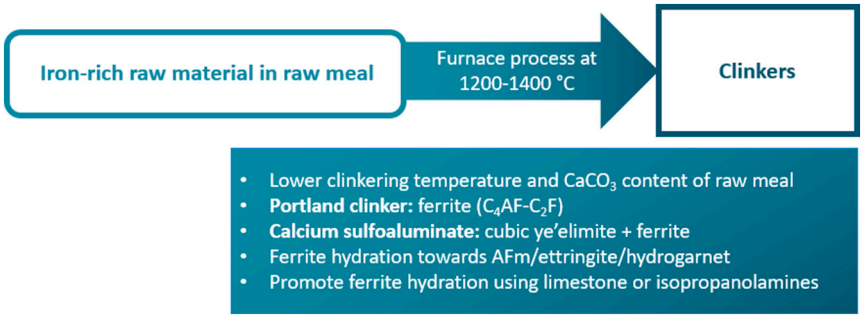

Fig. 6. Visual summary of Fe-rich cement clinkers. All raw materials from Section 2 can introduce iron into the system.

In the isopleth in Fig. 7, melting is shown at about 1400 °C. Above this a melt will form and become glassy; this is in fact a technique used by some in the metallurgical industry to make the slags environmentally friendly. As will be discussed in the following sections, the melting temperature in polyphase clinker systems differs than that of monophase systems. Indeed, these data need to be updated and critical databases parametrised and extended for clinker ferrite, melt, and polyphase systems, and including the minor elements which are found in Fe-rich residues (see Table 3). To simulate the cooling of clinker in thermodynamic models, the Scheil–Gulliver models/assumptions and modifications thereof can be used. The thermodynamic data of the hydration products of ferrites and in the presence of other clinker phases and mineral additives (e.g., limestone), also need to be further developed [172].

The cooling rate of clinker affects ferrite formation. Some older studies on the cooling rate of clinker (e.g. [175]) found amorphous phases forming in the Portland cement clinker, but some recent studies do not support this (e.g., [176]). This inconsistency may be due to a difference in cooling efficiency of different kilns or clinkers. Ichikawa et al. [177] showed that in slow cooled clinker, the F/A ratio in ferrite is higher than in quenched clinker. It must be noted that equilibrium cooling of the melt phase is hardly ever realised; therefore, making it essential to experimentally test the effects of cooling rates. Recent studies on cooling rate and ferrite tend to focus on the ye'elimite-rich systems rather than PC systems [178–180]. Dolenec et al. [180] recently showed that the cooling regime affected the mineralogy and morphology of the ferrite phase in calcium sulfoaluminate clinker. The lowest total amount of foreign ions in the ferrite was taken up in the slowly cooled clinker. Moreover, the F/A ratio changes with cooling rates and changes the reactivity, which generally decreases as the iron content increases [181].

Ferrite is a sink for Mg, Zn, and Ti [182,183]. Ti preferably goes into the interstitial phases in Portland cement clinker with the preference of $C_4AF > C_3A > C_2S > C_3S$ and can affect its microstructure [184]. With increasing levels of titanium, the ferrite phase progressively transitions from a brownmillerite to a perovskite-type structure with diminished reactivity [185]. Duvallet et al. [186] showed that even low dosages (few wt%) of TiO_2 in ferrite (monophase system) has significant effects on the microstructure and hydraulicity. The ferrite phase also incorporates Si, Na, and S [177,187] and the higher the amount of SiO_2, the higher the viscosity of the ferrite melt. The incorporation of SO_3 changes the physicochemical properties of the clinker melt [188]. The presence of Na_2O promotes the formation of C_3A and changes its crystal system while the resultant ferrite phase becomes higher in Fe_2O_3; the viscosity rise enabled by Na is also reported to promote equilibrium [189].

4.1.2. Fe-rich Portland cement clinker

Although PC has been developed over two centuries, the iron-containing component is the least studied out of the four major PC clinker phases (alite, belite, tricalcium aluminate, ferrite) [190]. Despite the low amount of studies on the ferrite phase, the addition of iron-rich raw materials is common practice in PC production. The drivers to increase the iron content of PC clinkers further are:

1) to lower the production temperature of cement clinker and improve the burnability and reaction through melt/flux formation [12,191,192];
2) to meet valorisation and landfill diversion targets to use iron bearing by-products, and/or
3) to limit the tricalcium aluminate content or alumina modulus (A/F) to increase sulphate resistance of the cement [11].

The effect of iron on the clinkering temperature is well-known and this is the main reason for which Fe-rich raw materials are nowadays added to the PC raw meal. For Portland clinkers with high iron content, the production temperature can be decreased to 1350 °C from the typical 1450 °C when the ferrite content is increased to 9.4 wt% at the expense of belite content in the resulting clinker [12]. This lower production temperature can be obtained because the formation of the melt phase during clinkering appears at lower temperatures and iron enhances alite formation, which is seen by the lower content/absence of free lime at lower clinkering temperatures [193]. No Fe substitution in hatrurite/alite is normally considered; however, recent synchrotron X-ray powder diffraction data by Fernandes et al. [194], who revised the structural model of the M1 polymorph, showed two interstitial sites for Fe^{3+} substitution up to limited saturation levels, but more work on the topic is required to fully reveal the saturation levels and their dependencies. The substitution of iron into the belite structure has been observed and modelled and linked to the inhibition or persistence of certain polymorphs [195–197].

The raw materials that are currently used to provide iron to the PC raw meal are various; a non-exhaustive list includes limonite, sludges, fly ashes, ferrosilicon, iron separated from slags, iron or steel fragments, and shot. Industrial residues are known to be already applied to this end, such as bauxite residue [66,85] or steel slag [77]. All materials from Section 2 have potential to be used to supply iron to the PC raw meal, when ignoring potential environmental problems. The energy requirements might change depending on the origin of the iron rich resource, due to potential oxidation (exothermic) or reduction (endothermic) reactions at the clinkering temperature. The F/A ratio and ferrite content in PC can be increased to mitigate degradation due to later ettringite formation via sulfate attack; maximum C_3A concentrations are defined in the EN 197-1:2011 when sulfate resistance is required. Therefore, sulfate resistant cements commonly have a higher iron content, and a ferrite content of more than 7 wt% is recommended when sulfate resistance is required [198,199].

The typical phases in hydrated iron-rich PC are portlandite, ettringite, AFm and hydrogarnet as well as amorphous phases (most importantly C-S-H) [193,200]. Hydrogarnet can form directly from C_2S and C_4AF hydration or from the hydration reaction of C_2S, C_4AF and strätlingite (which is only thermodynamically stable in high alumina systems) [200]. Iron can be incorporated into conventional hydrate phases by means of substitution into the crystal lattice. The maximum uptake of Fe^{3+} in C-S-H is very low (0.001 Fe^{3+}/Si) [201], due to the limited solubility of $Fe(OH)_3$, despite the strong sorption of Fe^{3+} to the C-S-H surface [201]. More common than the incorporation in C-S-H is the substitution of Fe^{3+} for Al^{3+} in the aluminate phases. Not only can Al^{3+} be substituted [202–204], but Fe^{3+} equivalents of the monosulfate, monocarbonate, and ettringite phases also exist [203,205,206]. The most thermodynamically stable phase for iron in hydrated Portland cement was shown to be siliceous hydrogarnet [207,208], although recent publications have raised the need to improve the accuracy and precision of the thermodynamic data that are incorporated in major databases used to predict the speciation of iron in hydrated cement [156].

An increase in ferrite content in PC normally leads to lower compressive strength in a straight comparison with C_3S, because the hydration rate of ferrite is much slower than of C_3S [193]. The hydration rate and products of ferrite are mainly controlled by the calcium sulfate content in the pore solution [209,210], although mixing limestone with PC and thus introducing carbonates to the system allows formation of hemicarbonate and monocarbonate AFm phases, enabling an enhancement of the reaction of the ferrite phase [211]. The hydration of the ferrite phase can also be enhanced by addition of triisopropanolamine (TIPA) [212] that is commonly used as a grinding agent. It is hypothesised that addition of TIPA leads to formation of ferric-alkanolamine complexes; alkanolamines, triethanolamine (TEA) and diethanol-isopropanolamine (DEIPA) have been found to have positive effect on hydration of ferrite phase [213]. TEA showed higher complexation with alumina, and DEIPA with iron. Both these additives primarily influenced the formation of ettringite.

4.1.3. Calcium sulfoaluminate(-ferrite) cement clinker

Calcium sulfoaluminate (CSA) based cements, which have a lower carbon footprint than PC [214], typically have ye'elimite ($C_4A_3\$$) and belite (C_2S) as major phases and are hydrated after blending with anhydrite (C$). In commercial CSA cements, the amount of ferrite phase is around 5 wt%. Some iron is present in the raw mix since the raw materials bauxite and clay always contain a minor amount of iron. Iron has both mineralising and fluxing effects on CSA clinkers and is therefore an important factor to predict the required clinkering temperature and dwell time for CSA mixes [215]. Fe^{3+} tends to substitute Al^{3+} in ye'elimite. Some of the recent studies have been focusing on the relationship between iron content in the raw mix and the iron content of the ye'elimite phase, and also to the formation of the ferrite phase [215–218]. With excess Fe^{3+} in a synthesis of ye'elimite, the maximum substitution level is reported to be around $x \approx 0.27$ or 8.8 wt% in $C_4A_{3-x}F_x\$$ [178,215]. However, a realistic incorporation level of iron into the ye'elimite phase in compositions relevant for CSA clinker is $x = 0.1$ or less [215]. Moreover, the Fe/Al ratio is shown to be lower in the slowly cooled sample compared to quenched and non-linearly cooled clinkers [180]. The iron content of ye'elimite in Fe-rich CSA mixes can also be adjusted by varying the CaO content [217]. In a CSA–C_4AF mix with 20 wt% C_4AF, a lower amount of CaO in the mix increased the incorporation of iron into the ye'elimite phase ($x \approx 0.37$ in $C_4A_{3-x}F_x\$$). Less C_2F/C_4AF can thus be formed because iron is located in the ye'elimite phase [217]. With higher firing temperature and longer holding time, the iron content of ye'elimite decreases and the content of ferrite phases (C_2F/C_4AF) increase [215,217]. High iron substitution levels change ye'elimite from an orthorhombic crystal structure towards cubic or pseudo-cubic [215,216,219]. Fe-rich cubic ye'elimite has faster hydration kinetics than iron-free orthorhombic ye'elimite [220].

The recent drive to incorporate more Fe-rich materials in cements has resulted in two new families of CSA cements [221]: so-called BYF (belite-ye'elimite-ferrite) and AYF (alite-ye'elimite-ferrite) cements; however, other names such as BCSAF are also used and there is no set nomenclature for these cements. A typical range of compositions of BYF cement clinker is 40–60 wt% belite (C_2S), 20–40 wt% ye'elimite ($C_4A_3\$$) and 5–45 wt% ferrite (C_4AF/C_2F) [217,222–224]. In AYF (alite-ye'elimite-ferrite) belite has been replaced (either partially or completely) with the main phase of PC cement, alite (C_3S) [225,226] and also here ferrite contents up to 45 wt% have been reported [227]. Using a fine-tuned chemical composition and dopants (F, Zn, B and Na), ye'elimite and alite can be produced below 1300 °C, which is 200–250 °C lower than the typical formation temperature of alite in production of PC clinker [226–228]. The optimal fluorine content to avoid unwanted phases in such systems was $0.075 \leq x \leq 0.15$ in $Ca_3Si_{1-x}Al_xO_{5-x}F_x$ [229]. Excess fluorine led to the formation of fluorellestadite that has poor hydraulic properties, whereas with too little fluorine, alite yield was low. A significant iron content – 20 wt% of ferrite – was necessary in the system to avoid unreacted raw materials such as CaO, $CaSO_4$ and Al_2O_3 [229]. The alite content can be increased from 12 to 24 wt% with the introduction of iron (going from alite-ye'elimite to alite-ye'elimite-ferrite cement) [225] - in other words, iron enhances alite formation in AYF clinkers.

The greatly reduced importance of phase composition or speciation of iron in the raw materials in determining the behaviour of the cement after clinkering and high potential ferrite content of CSA clinkers, makes the CSA clinkers an attractive route for the use of Fe-rich raw materials. In view of residue valorisation, many industrial residues and by-products from Section 2 are investigated to be incorporated in CSA clinker in high proportions with respect to the total raw meal. Bauxite residue [14,224,227,230], fayalitic slags [13,145,146] and jarosite sludges [231–233] have for instance been studied extensively.

4.1.4. Calcium aluminate cement clinker

Calcium aluminate cements (CACs) are the second overall in cement market volume, although far behind Portland cement [234]. These cements are known for rapid hardening and elevated chemical resistance towards sulfates, but above all, for a good retention of mechanical properties at high temperatures in comparison with Portland cement. Although they have use in construction and high water mine backfilling, refractory applications are mostly targeted by CAC producers. Several classes of CAC are distinguished based on the purity, mostly defined by the wt% of Al_2O_3 [234,235]. The most commercialised and most relevant to this review paper is the "Standard" grade CAC, which is the lowest in alumina content (36–42 wt% Al_2O_3) [234]. It can therefore incorporate the highest levels of iron (12–20 wt% of Fe_2O_3) [234,236], as it is intended for use at less-elevated temperature (whereas the higher-alumina CACs are used in higher-temperature refractory applications), and so the fluxing effect of the iron is not strongly detrimental to key performance characteristics. Similar to Portland cement, the iron is mostly present in the ferrite phase [234,235], but also in pleochroite [237]. Reducing conditions in the kiln during CAC production often result in the presence of minor contents of magnetite or wüstite in addition to the ferrite phase [234]. On top of the formation of Fe-rich phases, minor substitution of Fe^{2+} for Ca^{2+} in mayenite ($C_{12}A_7$) is observed [196]. This substitution does not occur to a significant extent in monocalcium aluminate (CA) or for Fe^{3+} [196].

The main hydration reactions in the CAC system result from the reactions of monocalcium aluminate (CA) and mayenite ($C_{12}A_7$) or grossite (CA_2) to form the calcium aluminate hydrates: CAH_{10}, C_2AH_8, C_3AH_6 and AH_3 [234,238]; however, only the latter two are stable at normal temperature and pressure. The presence of the ferrite phase results in a substitution of aluminium for iron in these hydrates and the formation of FH_3 [235], but less is known about the stability of the Fe-bearing hydrates.

4.2. Fe-rich supplementary cementitious materials

The decrease in clinker factor of cements (i.e., blending) using supplementary cementitious materials (SCMs) is an effective path to decrease CO_2 emissions of cement production in the short term [3,239]. This is due to the partial replacement of the CO_2-intensive clinker with (usually) CO_2-lean SCMs and the inclusion of conventional SCMs (GGBFS, coal combustion fly ash, natural pozzolans, and an increasing range of others) in cement and concrete technical standards to formulate blended cements. At present blended cements are dominating global cement markets. The term SCM covers mineral additions to cement that contribute to hydration by means of hydraulic or pozzolanic reactions [240]. Hydraulic SCMs, such as blast furnace slag, can react (slowly) with water to form low-solubility hydration products; their hydration can be accelerated by the addition of Portland cement to increase the alkalinity of the pore solution and provide an additional source of Ca. Pozzolanic materials, on the other hand, do not react significantly in combination with water; in order to form hydration products, they consume portlandite which is usually provided by the hydration of Portland cement. Fig. 8 provides a visual summary of the use of Fe-rich SCMs.

The best-known example of a pozzolanic material is siliceous coal combustion fly ash. In most industrialised nations, supplies of conventional SCMs are already largely used by cement producers, making further decreases in clinker factor difficult to achieve without tapping into new SCM sources [4]. Given the ongoing low-carbon transformation in the energy sector, nowadays in Europe and globally by 2050, the availability of coal fly ashes is expected to decrease in the short term in many countries [241]. At the same time, the supply of blast furnace slags may be impacted by increased recycling rates in the steel industry and changes in the primary steel production process to meet CO_2 emission reduction targets by 2050 [243]. Clearly, alternative SCMs need to step in; most of the Fe-rich resources in Section 2 have been studied as SCMs, but only smectite clays, volcanic ashes, steel slags and fayalitic non-ferrous slags can introduce iron into the binding phase if no pre-treatments are carried out that change the speciation of iron (Section 3).

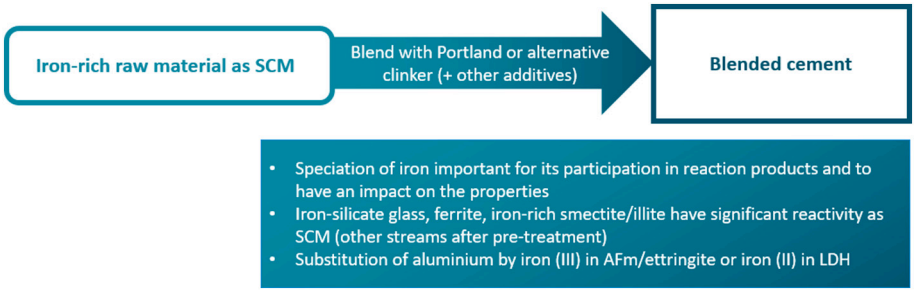

Fig. 8. Visual summary of Fe-rich SCMs and their roles in blends with Portland and other clinkers.

The reactivity of SCMs is an important characteristic as it relates to the contribution of the SCM to the development of mechanical and durability performance. To meet a lack in practical yet relevant reactivity test methods, RILEM TC 267-TRM developed a standard test method for the assessment of the chemical reactivity of conventional SCMs [244,245], the R3 test, which is now standardised as ASTM C1897. This reactivity test determines the inherent reactivity of the material, as measured in a model system consisting of a $Ca(OH)_2$ paste with minor additions of $CaCO_3$, KOH, and K_2SO_4. This model system simulates the reaction environment of the SCM in an actual cement mix, yet avoids interferences of the PC hydration in SCM-PC blends during the measurement. It ignores the impact the SCM might have on the reaction of the clinker phases. Reactive SCMs contribute to strength development, but in addition the formation of additional hydrate phases such as ettringite or AFm phases – which are relevant to Fe-containing SCMs - can enhance the durability of a hardened concrete by decreasing the permeability [246,247]. On the other hand, the consumption of Ca $(OH)_2$ in SCM hydration decreases the acid buffering capacity and can therefore decrease the carbonation resistance, which is important for reinforced concrete [19].

Specifically for aluminium-containing SCMs, the alkali-silica reaction is mitigated by the increased concentration of aluminium in the pore solution [248,249] and the associated decreased solubility of silica [250,251]. It is unknown whether Fe^{3+} can plan an analogous role to Al^{3+} in mitigating alkali-silica reactions, and this requires further investigation.

The reactivity of Fe-rich resources to form cementitious products can also be measured using the R3 test [15,89,108,109], but no confirmation of a quantitative reactivity-strength relation as for conventional SCMs is available as yet. Heat releases equivalent to those of siliceous coal combustion fly ashes can be obtained from resources containing Fe-rich silicate glasses (~200 J/g_{SCM} after 7 days at 40 °C; e.g. quenched fayalitic slags) [108,109], although not all reach this level [15,252]. The phase composition and involvement of iron in steel slags can be altered drastically by small chemical modifications or varying the cooling speed, reaching similar reactivity to coal fly ashes in terms of heat release after mixing with $Ca(OH)_2$ [82], although the contribution to strength development is often minor [80–82]. This lack in contribution to strength development is not seen for quenched fayalitic slags, which next to a significant reactivity can also show a contribution to strength development similar to coal fly ashes [15,108]. Furthermore, by engineering the particle size distribution and using a low water/binder ratio, no strength loss with respect to the reference Portland cement is observed [253]. The effect of the increased iron content in the binding phases and pore solution on the durability of the resultant concrete is not studied yet.

The incorporation of iron through the addition of SCMs to cement only slightly impacts the hydrate phase assemblage, as the main part of the binding phases derives from the reaction of the clinker phases. The speciation of Fe^{3+} in the cement hydrate phases was already discussed in the clinker section; however, Fe-rich SCMs can also contain Fe^{2+}. Fe^{2+} is prone to oxidation in alkaline conditions, but if stabilized, it can be incorporated in the C-S-H structure in an octahedral environment in the interlayer or on the surface [254]. Thermodynamic prediction have shown to be inaccurate in studies on the speciation of Fe^{2+}, which often predict the oxidation to Fe^{3+} and underestimate the solubility of Fe^{2+} [156]. When using a glassy fayalitic non-ferrous metallurgical slag as SCM, the major iron-containing hydrate phase was a layered double hydroxide including also aluminium and magnesium [16]. This iron was present as Fe^{2+} – the same oxidation state as in the slag – and thus did not oxidise before being incorporated into the hydrate phases [16]. Whether this phase is stable in the longer term, or if oxidation happens at later age (> 28 days), is not yet known, and any potential consequences regarding volume stability of the concrete also require further investigation.

4.3. Fe-rich alkali-activated materials

AAMs have the potential to substantially decrease the CO_2 emissions of cement production in the long term, if appropriate raw materials can be sourced. Estimations of the CO_2 decrease relative to CEM I based mortar or concrete range from 30% to 87% [255–259], depending on the exact formulation and the method of calculation. AAMs are commercially available in some countries, although there is not yet a breakthrough in global usage due to the misfit of these materials with prescriptive cement standards, and the conservatism of the construction sector when considering a new cementitious material with chemistry that is significantly different from Portland cement. The term AAMs encompasses binders generated by mixing (calcium/magnesium/alumino/ferro)silicate precursor powders with an alkaline activator [260]. The alkali activation pathway towards a hardened binder includes the dissolution of the solid precursor in the alkaline activator, followed by the precipitation of reaction products and/or the polymerisation of a silicate network. Starting from aluminosilicate precursors and if a silicate network is obtained in the hardened binder through polymerisation, a popular alternative name for the AAM is “geopolymer”.

The visual summary of this section about Fe-rich AAMs is shown in Fig. 9. The most common resources used to produce AAMs are the same conventional materials used as SCM: blast furnace slag, coal fly ash and metakaolin. This originates from the fact that the reactivity requirements are similar. The precursor has to dissolve in an alkaline environment and deliver silicate (and aluminate) species for the formation of the binder phase(s). The alkalinity of the alkaline activator is usually higher than that of the Portland cement pore solution, and therefore less reactive SCMs can also become candidates for use in AAMs. A detailed overview of several resources and their use in and value to AAMs was provided in a recent review paper [261].

Most AAMs have in common that the main binding phase consists of an alkali aluminosilicate network. In the case of Ca-poor precursors the final binder presents a zeolite-like alkali aluminosilicate network [262–264], sometimes described as N-A-S-H gel using cement notation [265,266]. When using Ca-rich precursors the binder is a calcium (alkali) aluminosilicate hydrate, C-(N-)A-S-H gel [265–268], sometimes accompanied by a small fraction of additional solid phases such as

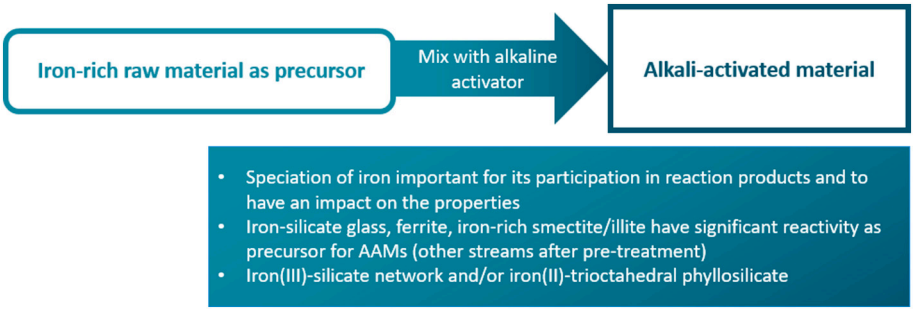

Fig. 9. Visual summary of Fe-rich SCMs. The involvement of iron from the raw materials from Section 2 depends on the speciation (Section 3).

Mg—Al and Ca—Al layered double hydroxides (such as AFm phases including strätlingite), or others [265,269,270].

The use of Fe-rich precursors for AAMs can significantly change the nanostructure of the binding phases in comparison with conventional (calcium) aluminosilicate AAMs. The difference is larger than for SCMs, simply due to the larger content of Fe-rich resource in an AAM blend than the content of SCM in a cement blend or the higher reaction extent of the Fe-rich precursor due to the higher alkalinity of the system. In other words, a high concentration of iron becomes available to end up in the binding phases, despite common assumptions that iron is not soluble at high pH. Although the latter might be true in pure Fe^{3+}-containing solutions, the presence of silicates and alkalis in solution and the fact that iron is also (or mostly) present as Fe^{2+}, results in significant solubilisation and participation in the reactions of iron. The resulting reaction products are amorphous; no crystalline Fe-rich phases have been observed in the literature.

The iron in AAM reaction products is at least partially in the Fe^{3+} oxidation state [157,271], even though Fe-rich resources often contain Fe^{2+}. The configuration of this Fe^{3+} is similar to Al in a N-A-S-H or C-A-S-H structure. When starting from Fe^{2+} silicate glasses, another part of the reaction products contains Fe^{2+} in octahedral configuration [271]. This Fe^{2+} is arranged in trioctahedral layers, commonly referred to in cement science as brucite-like layers [17], which is a similar structure as observed in trioctahedral phyllosilicates [114]. The role of minor calcium contents in Fe-rich resources on the binding phases is not yet clear, although a huge impact on the strength development is seen by comparing data from [153,161]. Part of the calcium goes into the trioctahedral layers [17], but it was theorised that the formation of C-S-H at later age is probable [114]. The Fe^{2+}-containing phyllosilicate-like structure is not stable in air; oxidation and a distortion of the structure is observed when samples are exposed to air as powder [17,18]. The Fe^{3+}-containing silicate network and the Fe^{2+}-containing phyllosilicate-like phase are formed simultaneously [271]. The amount of Fe^{3+} is driven by the availability of Na, as for most samples the Na^{+}/Fe^{3+} molar ratio decreases and converges to 1, after which only the formation of the Fe^{2+}-containing phyllosilicate-like structure continues [114,271].

The most commonly used activator for Fe-rich precursors has been NaOH or Na-silicate solutions [113,272,273]. The fresh properties of alkali-activated Fe-rich materials, such as setting time and early-age rheology, are highly dependent on the chosen type of precursor and activating solution. The setting time of iron silicate glass-based AAMs, e.g. AAMs from fayalitic slags, can be controlled from a few minutes to a few days by varying the SiO_2/Na_2O molar ratio of the sodium silicate activating solution [274–276], although the kinetics also depend on the chemical composition of the glass or the fraction of amorphous material [161,277]. The SiO_2/Na_2O molar ratio also has a slight effect on the early-age rheology of an iron silicate glass-based AAM paste [278], similar to conventional AAMs. However, strong particle interactions increase the yield stress of the fresh paste (in comparison with a quartz-activating solution mixture) [278].

To increase the compressive strength of AAMs including an Fe-rich resource, sometimes aluminosilicates such as fly ash can be added [279,280]. However, this is not needed in many cases, as the compressive strength of iron-silicate glass based AAMs is sufficient for structural purposes if adequate formulation and curing conditions are adopted [113,273,281,282] and high strengths can be obtained when low water/binder ratios are used [283]. Even fayalitic slag with a low amorphous content could be used as sole precursor in AAMs with adequate strength (~40 MPa after 28 days) after engineering the particle size distribution [112].

Studies related to the durability aspects of Fe-rich AAMs are scarce, considering the discussion on durability testing of conventional AAMs, but existing studies promise increased performance in harsh environments in comparison with Portland cement due to good resistance to sulfates [284], acids [285] and fire [286]. Being a completely different binder system, the testing methodology for assessing the durability of AAMs has to be carefully selected and is a subject of discussion [287–289]. The discussion on the test method is extrapolated towards the durability of the material, although studies of AAMs in existing structures in Ukraine, Belgium and other countries after multiple decades in service show that durable AAM-based concretes are certainly possible [290].

4.4. Limitations of this review regarding cement types

Sections 4.1–4.3 discussed the most abundantly researched cement types, for use on Earth, that incorporate Fe-rich raw materials. Other types exist as well, of which a brief discussion is provided in this section.

Acid-activated materials, carbonated products, and lime-pozzolan binders. The acid equivalent of alkali-activation commonly uses phosphoric acid [42,291] to transform a powdered precursor in a solid material. Research has been carried on Fe-rich raw materials [29,292], but there is a potential mismatch between the availability of the mentioned acid in comparison with needed volumes in construction.

Carbonation is usually carried out to store CO_2 in and produce construction materials from Ca and Mg-rich materials [293,294]. Steel slags are exceptionally good precursors for carbonation [295,296], although that is mainly associated with their Ca-content. $FeCO_3$-based products have recently been developed [297,298], but the application to the other raw materials of Section 2 remains unclear.

Lime-pozzolan binders were already used by the Romans and recently a surge of attention has come back to this binder system [299–301] especially as slaked lime may be produced with diminished CO_2 emissions [302,303]. Instead of combining Portland cement with an SCM, lime is mixed with an SCM, in a process that is very analogous to alkali activation. The hydration products therefore completely result from the reaction of $Ca(OH)_2$ with the SCM and this system thus requires high-quality SCMs as well, which can be the Fe-rich raw materials discussed in this paper.

5. Summary and recommendations for future research

Fe-rich raw materials and cements have been discussed and assessed in this paper. The importance of the characteristics of the raw materials has been identified as a crucial factor for economic use in certain cements, as well as any necessary pre-treatment or processing that may ameliorate its use in cements.

It is crucial to understand the mechanisms of iron-rich phase formation both during clinkerisation and hydration/hardening, as well as compositional variations under different processing conditions and environments. The reactivity of the iron-containing phases in raw materials used as SCM or as precursor for AAMs also needs much more investigation, particularly linking this to the resulting influence of iron on the reaction products and technical properties of the bound material.

The discussion presented in this paper shows that basic knowledge on the behaviour of Fe-rich raw materials in the discussed cement types exists. However, there is a long way to go, and many open research questions remain for all the cement systems. A few examples formulated as recommendations for future research and development are:

- Building machine-actionable databases of available raw materials, including Fe-rich phases, to provide a clear overview to the construction sector about the potential sources of raw materials
- Detailed regionalised assessment/compilation of Fe-rich wastes, providing information on any organic or calorific content as well as impurities (minor elements and any others that are not normal constituents of cement)
- Design of ferrite phases in cement clinker for improved performance
- Increased understanding of, and improvements in, the hydraulicity of ferrite and its interaction with other clinker phases
- Design and development of new clinkerisation processes and clinker formulations, as well as optimisation of existing processes in view of net-zero CO_2
- Development of economic pre-treatment and separation processes for raw materials that are currently not suited for cement production due to limited reactivity or elevated heavy metal concentrations
- Understanding of factors influencing reactivity of iron-rich resources as SCMs or AAM precursors, and establishment of reactivity vs. performance relationships
- Selection criteria for Fe-rich materials for sustainable clinker production and/or use as SCMs or in AAMs
- The effect of Fe-rich phases in clinkers on the comminution process
- Development of thermodynamic models for the ferrite phase and including in clinker systems and in the presence of other elements found in Fe-rich raw material streams
- Further knowledge on Fe-rich hydration and activation products, their molecular structure and stability, including kinetic and thermodynamic data
- The impact of dissolved Fe on fresh properties of mortars and concrete
- Development of chemical additives for Fe-rich cements
- Durability testing and developments of durability tests that take into account specific reactions of Fe-rich reaction products, and in particular the potential oxidation of iron(II)-containing phases
- Understanding the impact of Fe-rich reaction products on the durability of concrete
- Recycling of concretes with Fe-rich cements and the impact of the increased complexity of cements on the recyclability of concrete products
- Standardisation and go-to-market strategies of cements from new sources of raw materials

Declaration of competing interest

The authors declare that they have no known competing financial interests or personal relationships that could have appeared to influence the work reported in this paper.

Acknowledgements

T. Hanein was funded by UKRI Future Leaders Fellowship (MR/V023829/1). A. Yorkshire and J. L. Provis were funded by EPSRC (EP/T013524/1). J. L. Provis and T. Hanein were also funded by UKRI through the ICEC-MCM centre (EP/V011820/1). V. Isteri was funded by Business Finland project: Towards Carbon Neutral Metals – TOCANEM (No. 41700/31/2020).

Credit authorship contribution statement

Conceptualization: AP, TH
Writing - Original Draft: AP, VI, JY, ASY, PNL, RS, TH
Visualisation: AP
Software: CU
Writing - Review & Editing: AP, JLP, RS, TH

References

[1] F.W. Clarke, H.S. Washington, The Composition of the Earth's Crust; United States Geological Survey, Department of the Interior, Washington, 1924.
[2] A. Poldervaart, Chemistry of the Earth's crust, in: Proceedings of the Crust of the Earth: A Symposium, 1955, pp. 119–144.
[3] G. Habert, S.A. Miller, V.M. John, J.L. Provis, A. Favier, A. Horvath, K. L. Scrivener, Environmental impacts and decarbonization strategies in the cement and concrete industries, Nat. Rev. Earth Environ. 1 (2020) 559–573, https://doi.org/10.1038/s43017-020-0093-3.
[4] K.L. Scrivener, V.M. John, E.M. Gartner, in: Eco-efficient Cements: Potential, Economically Viable Solutions for a Low-CO2, Cement-based Materials Industry, United Nations Environment Programme, Paris, 2016, p. 50.
[5] N.M. Piatak, M.B. Parsons, R.R. Seal, Characteristics and environmental aspects of slag: a review, Appl. Geochem. 57 (2015) 236–266, https://doi.org/10.1016/j.apgeochem.2014.04.009.
[6] B. Gorai, R.K. Jana, Premchand. Characteristics and utilisation of copper slag—a review, Resour. Conserv. Recycl. 39 (2003) 299–313, https://doi.org/10.1016/s0921-3449(02)00171-4.
[7] Y. Pontikes, G.N. Angelopoulos, Bauxite residue in cement and cementitious applications: current status and a possible way forward, Resour. Conserv. Recycl. 73 (2013) 53–63, https://doi.org/10.1016/j.resconrec.2013.01.005.
[8] J. Spooren, K. Binnemans, J. Björkmalm, K. Breemersch, Y. Dams, K. Folens, M. González-Moya, L. Horckmans, K. Komnitsas, W. Kurylak, et al., Near-zero-waste processing of low-grade, complex primary ores and secondary raw materials in Europe: technology development trends, Resour. Conserv. Recycl. 160 (2020), 104919, https://doi.org/10.1016/j.resconrec.2020.104919.
[9] A.O. Babatunde, Y.Q. Zhao, Constructive approaches toward water treatment works sludge management: an international review of beneficial reuses, Crit. Rev. Environ. Sci. Technol. 37 (2007) 129–164, https://doi.org/10.1080/10643380600776239.
[10] B. Mysen, P. Richet, Chapter 11 - structure of iron silicate glasses and melts, in: B. Mysen, P. Richet (Eds.), Silicate Glasses and Melts, Second Edition, Elsevier, 2019, pp. 403–430.
[11] P. Hewlett, M. Liska, Lea's Chemistry of Cement and Concrete, Butterworth-Heinemann, 2019.
[12] Y. Elakneswaran, N. Noguchi, K. Matumoto, Y. Morinaga, T. Chabayashi, H. Kato, T. Nawa, Characteristics of ferrite-rich Portland cement: comparison with ordinary Portland cement, Front. Mater. 6 (2019) 97.
[13] V. Isteri, K. Ohenoja, T. Hanein, H. Kinoshita, P. Tanskanen, M. Illikainen, T. Fabritius, Production and properties of ferrite-rich CSAB cement from metallurgical industry residues, Sci. Total Environ. 712 (2020), 136208.
[14] T. Hertel, A. Van den Bulck, S. Onisei, P.P. Sivakumar, Y. Pontikes, Boosting the use of bauxite residue (red mud) in cement - production of an fe-rich calciumsulfoaluminate-ferrite clinker and characterisation of the hydration, Cem. Concr. Res. 145 (2021), 106463, https://doi.org/10.1016/j.cemconres.2021.106463.
[15] A. Gholizadeh Vayghan, L. Horckmans, R. Snellings, A. Peys, P. Teck, J. Maier, B. Friedrich, K. Klejnowska, Use of treated non-ferrous metallurgical slags as supplementary cementitious materials in cementitious mixtures, Appl. Sci. 11 (2021) 4028.
[16] V. Hallet, M.T. Pedersen, B. Lothenbach, F. Winnefeld, N. De Belie, Y. Pontikes, Hydration of blended cement with high volume iron-rich slag from non-ferrous metallurgy, Cem. Concr. Res. 151 (2022), 106624, https://doi.org/10.1016/j.cemconres.2021.106624.
[17] A. Peys, C.E. White, H. Rahier, B. Blanpain, Y. Pontikes, Alkali-activation of CaO-FeOx-SiO2 slag: formation mechanism from in-situ X-ray total scattering, Cem. Concr. Res. 122 (2019) 179–188, https://doi.org/10.1016/j.cemconres.2019.04.019.
[18] A. Peys, A.P. Douvalis, C. Siakati, H. Rahier, B. Blanpain, Y. Pontikes, The influence of air and temperature on the reaction mechanism and molecular

structure of fe-silicate inorganic polymers, J. Non-Cryst. Solids 526 (2019), 119675, https://doi.org/10.1016/j.jnoncrysol.2019.119675.
[19] K. Scrivener, F. Avet, H. Maraghechi, F. Zunino, J. Ston, W. Hanpongpun, A. Favier, Impacting factors and properties of limestone calcined clay cements (LC3), Green Mater. 7 (2019) 3–14, https://doi.org/10.1680/jgrma.18.00029.
[20] B.T. Kamtchueng, V.L. Onana, W.Y. Fantong, A. Ueda, R.F.D. Ntouala, M.H. D. Wongolo, G.B. Ndongo, A.N.O. Ze, V.K.B. Kamgang, J.M. Ondoa, Geotechnical, chemical and mineralogical evaluation of lateritic soils in humid tropical area (Mfou, Central-Cameroon): implications for road construction, Int. J. Geo-Eng. (6) (2015) 1, https://doi.org/10.1186/s40703-014-0001-0.
[21] A. Ito, R. Wagai, Global distribution of clay-size minerals on land surface for biogeochemical and climatological studies, Sci. Data 4 (2017), 170103.
[22] S. Nickovic, A. Vukovic, M. Vujadinovic, V. Djurdjevic, G. Pejanovic, C. Hoose, High-resolution mineralogical database of dust-productive soils for atmospheric dust modeling, Atmos. Chem. Phys. 12 (2012).
[23] R.C. Kaze, L.M. Beleuk à Moungam, M.L. Fonkwe Djouka, A. Nana, E. Kamseu, U. F. Chinje Melo, C. Leonelli, The corrosion of kaolinite by iron minerals and the effects on geopolymerization, Appl. Clay Sci. 138 (2017) 48–62, https://doi.org/10.1016/j.clay.2016.12.040.
[24] M.M. Mestdagh, L. Vielvoye, A.J. Herbillon, Iron in kaolinite: II. The relationship between kaolinite crystallinity and iron content, Clay Miner. 15 (1980) 1–13, https://doi.org/10.1180/claymin.1980.015.1.01.
[25] B. Lorentz, N. Shanahan, Y.P. Stetsko, A. Zayed, Characterization of Florida kaolin clays using multiple-technique approach, Appl. Clay Sci. 161 (2018) 326–333.
[26] S. Hollanders, R. Adriaens, J. Skibsted, Ö. Cizer, J. Elsen, Pozzolanic reactivity of pure calcined clays, Appl. Clay Sci. 132 (2016) 552–560.
[27] C. Bich, J. Ambroise, J. Péra, Influence of degree of dehydroxylation on the pozzolanic activity of metakaolin, Appl. Clay Sci. 44 (2009) 194–200, https://doi.org/10.1016/j.clay.2009.01.014.
[28] G. Kakali, T. Perraki, S. Tsivilis, E. Badogiannis, Thermal treatment of kaolin: the effect of mineralogy on the pozzolanic activity, Appl. Clay Sci. 20 (2001) 73–80.
[29] C.R. Kaze, G.L. Lecomte-Nana, E. Kamseu, P.S. Camacho, A.S. Yorkshire, J. L. Provis, M. Duttine, A. Wattiaux, U.C. Melo, Mechanical and physical properties of inorganic polymer cement made of iron-rich laterite and lateritic clay: a comparative study, Cem. Concr. Res. 140 (2021), 106320, https://doi.org/10.1016/j.cemconres.2020.106320.
[30] A.Z. Khalifa, Ö. Cizer, Y. Pontikes, A. Heath, P. Patureau, S.A. Bernal, A.T. Marsh, Advances in alkali-activation of clay minerals, Cem. Concr. Res. 132 (2020), 106050.
[31] T. Danner, G. Norden, H. Justnes, Calcareous smectite clay as a pozzolanic alternative to kaolin, Eur. J. Environ. Civ. Eng. (2019) 1–18.
[32] T. Danner, G. Norden, H. Justnes, Characterisation of calcined raw clays suitable as supplementary cementitious materials, Appl. Clay Sci. 162 (2018) 391–402.
[33] C. Rodrigue Kaze, P. Ninla Lemougna, T. Alomayri, H. Assaedi, A. Adesina, S. Kumar Das, G.-L. Lecomte-Nana, E. Kamseu, U. Chinje Melo, C. Leonelli, Characterization and performance evaluation of laterite based geopolymer binder cured at different temperatures, Constr. Build. Mater. 270 (2021), 121443, https://doi.org/10.1016/j.conbuildmat.2020.121443.
[34] J.W. Stucki, Properties and behaviour of iron in clay minerals, in: Developments in Clay Science Volume 5, Elsevier, 2013, pp. 559–611.
[35] A.G. Ilgen, R.K. Kukkadapu, K. Leung, R.E. Washington, "Switching on" iron in clay minerals, Environ. Sci.: Nano 6 (2019) 1704–1715.
[36] European Dredging Association, Dredged Material & Environmental Regulation in EU, EuDA Publications, 2005.
[37] R. Snellings, Ö. Cizer, L. Horckmans, P.T. Durdziński, P. Dierckx, P. Nielsen, K. Van Balen, L. Vandewalle, Properties and pozzolanic reactivity of flash calcined dredging sediments, Appl. Clay Sci. 129 (2016) 35–39, https://doi.org/10.1016/j.clay.2016.04.019.
[38] M. Benzerzour, M. Amar, N.-E. Abriak, New experimental approach of the reuse of dredged sediments in a cement matrix by physical and heat treatment, Constr. Build. Mater. 140 (2017) 432–444.
[39] M. Amar, M. Benzerzour, J. Kleib, N.-E. Abriak, From dredged sediment to supplementary cementitious material: characterization, treatment, and reuse, Int. J. Sediment Res. 36 (2021) 92–109, https://doi.org/10.1016/j.ijsrc.2020.06.002.
[40] A. Bouchikhi, W. Maherzi, M. Benzerzour, Y. Mamindy-Pajany, A. Peys, N.-E. Abriak, Manufacturing of low-carbon binders using waste glass and dredged sediments: formulation and performance assessment at laboratory scale, Sustainability 13 (2021) 4960.
[41] H. Slimanou, K. Bouguermouh, N. Bouzidi, Synthesis of geopolymers based on dredged sediment in calcined and uncalcined states, Mater. Lett. 251 (2019) 188–191, https://doi.org/10.1016/j.matlet.2019.05.070.
[42] M. Lassinantti Gualtieri, M. Romagnoli, S. Pollastri, A.F. Gualtieri, Inorganic polymers from laterite using activation with phosphoric acid and alkaline sodium silicate solution: mechanical and microstructural properties, Cem. Concr. Res. 67 (2015) 259–270, https://doi.org/10.1016/j.cemconres.2014.08.010.
[43] A. Alujas, R. Fernández, R. Quintana, K.L. Scrivener, F. Martirena, Pozzolanic reactivity of low grade kaolinitic clays: influence of calcination temperature and impact of calcination products on OPC hydration, Appl. Clay Sci. 108 (2015) 94–101, https://doi.org/10.1016/j.clay.2015.01.028.
[44] A. McIntosh, S.E.M. Lawther, J. Kwasny, M.N. Soutsos, D. Cleland, S. Nanukuttan, Selection and characterisation of geological materials for use as geopolymer precursors, Adv. Appl. Ceram. 114 (2015) 378–385, https://doi.org/10.1179/1743676115Y.0000000055.
[45] E.F. Irassar, V.L. Bonavetti, C.C. Castellano, M.A. Trezza, V.F. Rahhal, G. Cordoba, R. Lemma, Calcined illite-chlorite shale as supplementary cementing material: thermal treatment, grinding, color and pozzolanic activity, Appl. Clay Sci. 179 (2019), 105143.
[46] A. Játiva, E. Ruales, M. Etxeberria, Volcanic ash as a sustainable binder material: an extensive review, Materials (2021) 14, https://doi.org/10.3390/ma14051302.
[47] R. Siddique, Effect of volcanic ash on the properties of cement paste and mortar, Resour. Conserv. Recycl. 56 (2011) 66–70, https://doi.org/10.1016/j.resconrec.2011.09.005.
[48] P.N. Lemougna, K.-T. Wang, Q. Tang, A.N. Nzeukou, N. Billong, U.C. Melo, X.-M. Cui, Review on the use of volcanic ashes for engineering applications, Resour. Conserv. Recycl. 137 (2018) 177–190, https://doi.org/10.1016/j.resconrec.2018.05.031.
[49] G. Cai, T. Noguchi, H. Degée, J. Zhao, R. Kitagaki, Volcano-related materials in concretes: a comprehensive review, Environ. Sci. Pollut. Res. 23 (2016) 7220–7243, https://doi.org/10.1007/s11356-016-6161-z.
[50] T. Ohba, M. Nakagawa, Minerals in volcanic ash 2: non-magmatic minerals, Glob. Environ. Res. 6 (2002) 53–60.
[51] G. Mertens, R. Snellings, K. Van Balen, B. Bicer-Simsir, P. Verlooy, J. Elsen, Pozzolanic reactions of common natural zeolites with lime and parameters affecting their reactivity, Cem. Concr. Res. 39 (2009) 233–240, https://doi.org/10.1016/j.cemconres.2008.11.008.
[52] K. Kupwade-Patil, M. Tyagi, C.M. Brown, O. Büyüköztürk, Water dynamics in cement paste at early age prepared with pozzolanic volcanic ash and ordinary Portland cement using quasielastic neutron scattering, Cem. Concr. Res. 86 (2016) 55–62, https://doi.org/10.1016/j.cemconres.2016.04.011.
[53] S. Al-Fadala, J. Chakkamalayath, S. Al-Bahar, A. Al-Aibani, S. Ahmed, Significance of performance based specifications in the qualification and characterization of blended cement using volcanic ash, Constr. Build. Mater. 144 (2017) 532–540, https://doi.org/10.1016/j.conbuildmat.2017.03.180.
[54] R. Snellings, G. Mertens, Ö. Cizer, J. Elsen, Early age hydration and pozzolanic reaction in natural zeolite blended cements: reaction kinetics and products by in situ synchrotron X-ray powder diffraction, Cem. Concr. Res. 40 (2010) 1704–1713.
[55] J.N.Y. Djobo, A. Elimbi, H.K. Tchakouté, S. Kumar, Reactivity of volcanic ash in alkaline medium, microstructural and strength characteristics of resulting geopolymers under different synthesis conditions, J. Mater. Sci. 51 (2016) 10301–10317, https://doi.org/10.1007/s10853-016-0257-1.
[56] S. Zhou, C. Lu, X. Zhu, F. Li, Upcycling of natural volcanic resources for geopolymer: comparative study on synthesis, reaction mechanism and rheological behavior, Constr. Build. Mater. 268 (2021), 121184, https://doi.org/10.1016/j.conbuildmat.2020.121184.
[57] K. Celik, M.D. Jackson, M. Mancio, C. Meral, A.H. Emwas, P.K. Mehta, P.J. M. Monteiro, High-volume natural volcanic pozzolan and limestone powder as partial replacements for Portland cement in self-compacting and sustainable concrete, Cem. Concr. Compos. 45 (2014) 136–147, https://doi.org/10.1016/j.cemconcomp.2013.09.003.
[58] P.N. Lemougna, U.F. Chinje Melo, M.-P. Delplancke, H. Rahier, Influence of the chemical and mineralogical composition on the reactivity of volcanic ashes during alkali activation, Ceram. Int. 40 (2014) 811–820, https://doi.org/10.1016/j.ceramint.2013.06.072.
[59] D. Bondar, C.J. Lynsdale, N.B. Milestone, N. Hassani, A.A. Ramezanianpour, Effect of heat treatment on reactivity-strength of alkali-activated natural pozzolans, Constr. Build. Mater. 25 (2011) 4065–4071, https://doi.org/10.1016/j.conbuildmat.2011.04.044.
[60] K.M.A. Hossain, Volcanic ash and pumice as cement additives: pozzolanic, alkali-silica reaction and autoclave expansion characteristics, Cem. Concr. Res. 35 (2005) 1141–1144, https://doi.org/10.1016/j.cemconres.2004.09.025.
[61] T. Gao, T. Dai, L. Shen, L. Jiang, Benefits of using steel slag in cement clinker production for environmental conservation and economic revenue generation, J. Clean. Prod. 282 (2021), 124538.
[62] H. Yi, G. Xu, H. Cheng, J. Wang, Y. Wan, H. Chen, An overview of utilization of steel slag, Procedia Environ. Sci. 16 (2012) 791–801, https://doi.org/10.1016/j.proenv.2012.10.108.
[63] World Steel Association, World Steel in Figures, 2021. Available online: https://worldsteel.org/.
[64] C. Liu, BOF Slag Hot-stage Engineering Towards Iron Recovery and use as Binders. Doctoral Thesis, KU Leuven, 2017.
[65] T. Gao, T. Dai, L. Shen, L. Jiang, Benefits of using steel slag in cement clinker production for environmental conservation and economic revenue generation, J. Clean. Prod. 282 (2021), 124538, https://doi.org/10.1016/j.jclepro.2020.124538.
[66] K. Evans, The history, challenges, and new developments in the management and use of bauxite residue, J. Sustain. Metall. 2 (2016) 316–331, https://doi.org/10.1007/s40831-016-0060-x.
[67] I.T. Burke, W.M. Mayes, C.L. Peacock, A.P. Brown, A.P. Jarvis, K. Gruiz, Speciation of arsenic, chromium, and vanadium in red mud samples from the Ajka spill site, Hungary, Environ. Sci. Technol. 46 (2012) 3085–3092, https://doi.org/10.1021/es3003475.
[68] A. Pappu, M. Saxena, S.R. Asolekar, Jarosite characteristics and its utilisation potentials, Sci. Total Environ. 359 (2006) 232–243.
[69] B.P. Wilson, P. Halli, I. Orko, P. Kangas, M. Lundström, P. Koukkari, Value-added Materials From the Hydrometallurgical Processing of Jarosite Waste. E3S Web of Conferences (Vol. 8)., EDP Sciences, 2016.
[70] E. Van Genderen, M. Wildnauer, N. Santero, N. Sidi, A global life cycle assessment for primary zinc production, Int. J. Life Cycle Assess. 21 (2016) 1580–1593, https://doi.org/10.1007/s11367-016-1131-8.

[71] S. De Carvalho Gomes, J.L. Zhou, W. Li, G. Long, Progress in manufacture and properties of construction materials incorporating water treatment sludge: a review, Resour. Conserv. Recycl. 145 (2019) 148–159, https://doi.org/10.1016/j.resconrec.2019.02.032.

[72] A.S. Brand, E.O. Fanijo, A review of the influence of steel furnace slag type on the properties of cementitious composites, Appl. Sci. 10 (2020) 8210.

[73] H. Nguyen, P. Kinnunen, K. Gijbels, V. Carvelli, H. Sreenivasan, A.M. Kantola, V.-V. Telkki, W. Schroeyers, M. Illikainen, Ettringite-based binder from ladle slag and gypsum – the effect of citric acid on fresh and hardened state properties, Cem. Concr. Res. 123 (2019), 105800, https://doi.org/10.1016/j.cemconres.2019.105800.

[74] B.o.I Recycling, World Steel Recycling in Figures 2015-2019: Steel Scrap - A Raw Material for Steelmaking; Brussels, Belgium, 2020.

[75] International Stainless Steel Forum (ISSF), Stainless steel meltshop production, Available online: https://www.worldstainless.org/statistics/stainless-steel-meltshop-production/stainless-steel-meltshop-production-2014-2020/, 2014-2020.

[76] A.L. Riley, J.M. MacDonald, I.T. Burke, P. Renforth, A.P. Jarvis, K.A. Hudson-Edwards, J. McKie, W.M. Mayes, Legacy iron and steel wastes in the UK: extent, resource potential, and management futures, J. Geochem. Explor. 219 (2020), 106630, https://doi.org/10.1016/j.gexplo.2020.106630.

[77] C. De Groot, R. Schoofs, J. Van Roo, M. Vervaet, D. Dedecker, K. Smeets, P. Dierckx, K. Broos, P. Nielsen, L. Van den Abeele, in: Monitoringsysteem duurzaam oppervlaktedelfstoffenbeleid. Inzet primarie delfstoffen en alternatieve grondstoffen in Vlaanderen in 2015.; D/2017/3241/377, Departement Omgeving, OVAM, VITO, Brussel, 2017, p. 155.

[78] R.I. Iacobescu, Y. Pontikes, D. Koumpouri, G.N. Angelopoulos, Synthesis, characterization and properties of calcium ferroaluminate belite cements produced with electric arc furnace steel slag as raw material, Cem. Concr. Compos. 44 (2013) 1–8.

[79] D. Adolfsson, N. Menad, E. Viggh, B. Björkman, Steelmaking slags as raw material for sulphoaluminate belite cement, Adv. Cem. Res. 19 (2007) 147–156, https://doi.org/10.1680/adcr.2007.19.4.147.

[80] A. Mladenovič, B. Mirtič, A. Meden, V. Zalar Serjun, Calcium aluminate rich secondary stainless steel slag as a supplementary cementitious material, Constr. Build. Mater. 116 (2016) 216–225, https://doi.org/10.1016/j.conbuildmat.2016.04.141.

[81] S. Fathy, G. Liping, R. Ma, G. Chunping, S. Wei, Comparison of hydration properties of cement-carbon steel slag and cement-stainless steel slag blended binder, Adv. Mater. Sci. Eng. 2018 (2018), 1851367, https://doi.org/10.1155/2018/1851367.

[82] Y. Wang, P. Suraneni, Experimental methods to determine the feasibility of steel slags as supplementary cementitious materials, Constr. Build. Mater. 204 (2019) 458–467, https://doi.org/10.1016/j.conbuildmat.2019.01.196.

[83] Y. Jiang, T.-C. Ling, C. Shi, S.-Y. Pan, Characteristics of steel slags and their use in cement and concrete—a review, Resour. Conserv. Recycl. 136 (2018) 187–197.

[84] P.L. Lopez Gonzalez, R.M. Novais, J.A. Labrincha, B. Blanpain, Y. Pontikes, Modifications of basic-oxygen-furnace slag microstructure and their effect on the rheology and the strength of alkali-activated binders, Cem. Concr. Compos. 97 (2019) 143–153, https://doi.org/10.1016/j.cemconcomp.2018.12.013.

[85] C. Klauber, M. Gräfe, G. Power, in: Review of Bauxite Residue "Re-use" Options, CSIRO Minerals, Waterford, WA, 2009, pp. 1–77.

[86] Interna6tional Aluminium Institute, World aluminium - statistics, Available online: https://international-aluminium.org/statistics/primary-aluminium-production/.

[87] S. Patel, B.K. Pal, Current status of an industrial waste: red mud an overview, International Journal of Latest Technology in Engineering, Management & Applied Science 4 (8) (2015) 1–16.

[88] G. Moise, P. Capota, L. Enache, E. Neagu, V. Dragut, D. Mihaescu, L. Mara, A. Chirea, R. Zavoianu, A. Sarbu, Material Composition and Properties of Red Mud Coming From Domestic Alumina Processing Plant. Proceedings: International symposium "The environment and the industry", SIMI 2017, 2017.

[89] T. Danner, H. Justnes, Bauxite residue as supplementary cementitious material – efforts to reduce the amount of soluble sodium, Nordic Concr. Res. 62 (2020) 1–20, https://doi.org/10.2478/ncr-2020-0001.

[90] E.P. Manfroi, M. Cheriaf, J.C. Rocha, Microstructure, mineralogy and environmental evaluation of cementitious composites produced with red mud waste, Constr. Build. Mater. 67 (2014) 29–36.

[91] D.V. Ribeiro, J.A. Labrincha, M.R. Morelli, Use of red mud as addition for Portland cement mortars, J. Mater. Sci. Eng. 4 (2010).

[92] R.C.O. Romano, H.M. Bernardo, M.H. Maciel, R.G. Pileggi, M.A. Cincotto, Hydration of Portland cement with red mud as mineral addition, J. Therm. Anal. Calorim. 131 (2018) 2477–2490, https://doi.org/10.1007/s10973-017-6794-2.

[93] M. Serdar, I. Biljecki, D. Bjegović, High-performance concrete incorporating locally available industrial by-products, J. Mater. Civ. Eng. 29 (2017), 04016239, https://doi.org/10.1061/(ASCE)MT.1943-5533.0001773.

[94] C. Venkatesh, N. Ruben, M.S.R. Chand, Red mud as an additive in concrete: comprehensive characterization, J. Korean Ceram. Soc. 57 (2020) 281–289, https://doi.org/10.1007/s43207-020-00030-3.

[95] T. Hertel, S. Onisei, P.P. Sivakumar, Y. Pontikes, Pozzolanic activity of thermally treated bauxite residue in blends with ordinary portland cement, in: Proceedings of the Proceedings of the 5th International Slag Valorisation Symposium, 2017, pp. 267–270.

[96] T. Hertel, B. Blanpain, Y. Pontikes, A proposal for a 100 % use of bauxite residue towards inorganic polymer mortar, J. Sustain. Metall. 2 (2016) 394–404, https://doi.org/10.1007/s40831-016-0080-6.

[97] P.J. Joyce, T. Hertel, A. Goronovski, A.H. Tkaczyk, Y. Pontikes, A. Björklund, Identifying hotspots of environmental impact in the development of novel inorganic polymer paving blocks from bauxite residue, Resour. Conserv. Recycl. 138 (2018) 87–98.

[98] X. Ke, S.A. Bernal, N. Ye, J.L. Provis, J. Yang, One-part geopolymers based on thermally treated red Mud/NaOH blends, J. Am. Ceram. Soc. 98 (2015) 5–11, https://doi.org/10.1111/jace.13231.

[99] T. Hertel, Y. Pontikes, Geopolymers, inorganic polymers, alkali-activated materials and hybrid binders from bauxite residue (red mud) – putting things in perspective, J. Clean. Prod. 258 (2020), 120610, https://doi.org/10.1016/j.jclepro.2020.120610.

[100] Mining Technology, Global copper production to recover by 5.6% in 2021, after Covid-19 hit output in 2020, Available online, https://www.mining-technology.com/comment/global-copper-production-to-recover/.

[101] M. Garside, Copper - statistics & facts. https://www.statista.com/topics/1409/copper/, 2021.

[102] International Copper Association, Copper Recycling, Copper Alliance, 2014.

[103] M. Garside, Refinery production of copper worldwide from 2000 to 2019, Available online, https://www.statista.com/statistics/254917/total-global-copper-production-since-2006/.

[104] Statista Research Department, Global production of refined secondary copper from 2004 to 2019. https://www.statista.com/statistics/281022/global-production-of-refined-secondary-copper/.

[105] M. Garside, Nickel - statistics & facts. https://www.statista.com/topics/1572/nickel/.

[106] Nickel Institute, About nickel, Available online: https://nickelinstitute.org/about-nickel/.

[107] International Tin Association, Sustainable production, Available online: https://www.internationaltin.org/sustainable-production/.

[108] V. Hallet, N. De Belie, Y. Pontikes, The impact of slag fineness on the reactivity of blended cements with high-volume non-ferrous metallurgy slag, Constr. Build. Mater. 257 (2020), 119400, https://doi.org/10.1016/j.conbuildmat.2020.119400.

[109] P.P. Sivakumar, S. Matthys, N. De Belie, E. Gruyaert, Reactivity assessment of modified ferro silicate slag by R3 method, Appl. Sci. 11 (2021) 366.

[110] R.I. Iacobescu, V. Cappuyns, T. Geens, L. Kriskova, S. Onisei, P.T. Jones, Y. Pontikes, The influence of curing conditions on the mechanical properties and leaching of inorganic polymers made of fayalitic slag, Front. Chem. Sci. Eng. 11 (2017) 317–327, https://doi.org/10.1007/s11705-017-1622-6.

[111] K. Komnitsas, G. Bartzas, V. Karmali, E. Petrakis, W. Kurylak, G. Pietek, J. Kanasiewicz, Assessment of alkali activation potential of a polish ferronickel slag, Sustainability 11 (1863) (2019), 1863, https://doi.org/10.3390/su11071863.

[112] A. Adediran, J. Yliniemi, M. Illikainen, Development of sustainable alkali-activated mortars using Fe-rich fayalitic slag as the sole solid precursor, Front. Built Environ. (2021) 7, https://doi.org/10.3389/fbuil.2021.653466.

[113] K. Komnitsas, L. Yurramendi, G. Bartzas, V. Karmali, E. Petrakis, Factors affecting co-valorization of fayalitic and ferronickel slags for the production of alkali activated materials, Sci. Total Environ. 721 (2020), 137753, https://doi.org/10.1016/j.scitotenv.2020.137753.

[114] C. Siakati, A.P. Douvalis, V. Hallet, A. Peys, Y. Pontikes, Influence of CaO/FeO ratio on the formation mechanism and properties of alkali-activated fe-rich slags, Cem. Concr. Res. 146 (2021), 106466, https://doi.org/10.1016/j.cemconres.2021.106466.

[115] A.J. Monhemius, The iron elephant: a brief history of hydrometallurgists' struggles with element no. 26, CIM J. (2017) 8, https://doi.org/10.15834/cimj.2017.21.

[116] M.R.C. Ismael, J.M.R. Carvalho, Iron recovery from sulphate leach liquors in zinc hydrometallurgy, Miner. Eng. 16 (2003) 31–39, https://doi.org/10.1016/S0892-6875(02)00310-2.

[117] U.S.G. Survey, Zinc, 2021.

[118] K. Verscheure, M. Van Camp, B. Blanpain, P. Wollants, P. Hayes, E. Jak, Continuous fuming of zinc-bearing residues: part II. The submerged-plasma zinc-fuming process, Metall. Mater. Trans. B 38 (2007) 21–33, https://doi.org/10.1007/s11663-006-9010-5.

[119] A. Di Maria, K. Van Acker, Turning industrial residues into resources: an environmental impact assessment of goethite valorization, Engineering 4 (2018) 421–429, https://doi.org/10.1016/j.eng.2018.05.008.

[120] N. Rodriguez Rodriguez, L. Machiels, B. Onghena, J. Spooren, K. Binnemans, Selective recovery of zinc from goethite residue in the zinc industry using deep-eutectic solvents, RSC Adv. 10 (2020) 7328–7335, https://doi.org/10.1039/d0ra00277a.

[121] M. Pelino, C. Cantalini, C. Abbruzzese, P. Plescia, Treatment and recycling of goethite waste arising from the hydrometallurgy of zinc, Hydrometallurgy 40 (1996) 25–35, https://doi.org/10.1016/0304-386X(95)00004-Z.

[122] M. Wołowiec, A. Pruss, M. Komorowska-Kaufman, I. Lasocka-Gomuła, G. Rzepa, T. Bajda, The properties of sludge formed as a result of coagulation of backwash water from filters removing iron and manganese from groundwater, SN Appl. Sci. 1 (2019) 639, https://doi.org/10.1007/s42452-019-0653-7.

[123] C. Sullivan, M. Tyrer, C.R. Cheeseman, N.J. Graham, Disposal of water treatment wastes containing arsenic - a review, Sci. Total Environ. 408 (2010) 1770–1778, https://doi.org/10.1016/j.scitotenv.2010.01.010.

[124] P. Sylvester, T. Milner, J. Jensen, Radioactive liquid waste treatment at Fukushima daiichi, J. Chem. Technol. Biotechnol. 88 (2013) 1592–1596, https://doi.org/10.1002/jctb.4141.

[125] J. Maroušek, V. Stehel, M. Vochozka, L. Kolář, A. Maroušková, O. Strunecký, J. Peterka, M. Kopecký, S. Shreedhar, Ferrous sludge from water clarification: changes in waste management practices advisable, J. Clean. Prod. 218 (2019) 459–464, https://doi.org/10.1016/j.jclepro.2019.02.037.
[126] J. Lehto, R. Koivula, H. Leinonen, E. Tusa, R. Harjula, Removal of radionuclides from Fukushima Daiichi waste effluents, Sep. Purif. Rev. 48 (2019) 122–142, https://doi.org/10.1080/15422119.2018.1549567.
[127] S.D.C. Gomes, J.L. Zhou, W. Li, F. Qu, Recycling of raw water treatment sludge in cementitious composites: effects on heat evolution, compressive strength and microstructure, Resour. Conserv. Recycl. 161 (2020), https://doi.org/10.1016/j.resconrec.2020.104970.
[128] A. Roy, C.M. van Genuchten, I. Mookherjee, A. Debsarkar, A. Dutta, Concrete stabilization of arsenic-bearing iron sludge generated from an electrochemical arsenic remediation plant, J. Environ. Manag. 233 (2019) 141–150, https://doi.org/10.1016/j.jenvman.2018.11.062.
[129] A. Telesca, N. Ibris, M. Marroccoli, Use of potabilized water sludge in the production of low-energy blended calcium sulfoaluminate cements, Appl. Sci. 11 (2021) 1679.
[130] N.C. Collier, N.B. Milestone, J. Hill, I.H. Godfrey, Immobilisation of fe floc: part 2, encapsulation of floc in composite cement, J. Nucl. Mater. 393 (2009) 92–101, https://doi.org/10.1016/j.jnucmat.2009.05.010.
[131] N.C. Collier, N.B. Milestone, J. Hill, I.H. Godfrey, Immobilisation of fe floc: part 1, pre-treatment of floc with slaked lime, J. Nucl. Mater. 393 (2009) 77–86, https://doi.org/10.1016/j.jnucmat.2009.05.008.
[132] H.A. van der Sloot, Comparison of the characteristic leaching behavior of cements using standard (EN 196–1) cement mortar and an assessment of their long-term environmental behavior in construction products during service life and recycling, Cem. Concr. Res. 30 (2000) 1079–1096, https://doi.org/10.1016/S0008-8846(00)00287-8.
[133] H.A. van der Sloot, D.S. Kosson, N. Impens, N. Vanhoudt, T. Almahayni, H. Vandenhove, L. Sweeck, R. Wiegers, J.L. Provis, C. Gascó, 8 - Leaching assessment as a component of environmental safety and durability analyses for NORM containing building materials, in: W. Schroeyers (Ed.), Naturally Occurring Radioactive Materials in Construction, Woodhead Publishing, 2017, pp. 253–288.
[134] S. Paria, P.K. Yuet, Solidification–stabilization of organic and inorganic contaminants using Portland cement: a literature review, Environ. Rev. 14 (2006) 217–255, https://doi.org/10.1139/a06-004.
[135] F.P. Glasser, Immobilisation potential of cementious materials, in: J.J.J. M. Goumans, H.A. van der Sloot, T.G. Aalbers (Eds.), Studies in Environmental Science Volume 60, Elsevier, 1994, pp. 77–86.
[136] Q.Y. Chen, M. Tyrer, C.D. Hills, X.M. Yang, P. Carey, Immobilisation of heavy metal in cement-based solidification/stabilisation: a review, Waste Manag. 29 (2009) 390–403, https://doi.org/10.1016/j.wasman.2008.01.019.
[137] B.J. Zhan, J.-S. Li, D.X. Xuan, C.S. Poon, Recycling hazardous textile effluent sludge in cement-based construction materials: physicochemical interactions between sludge and cement, J. Hazard. Mater. 381 (2020), 121034, https://doi.org/10.1016/j.jhazmat.2019.121034.
[138] L. Liu, L. Wang, S. Su, T. Yang, Z. Dai, M. Qing, K. Xu, S. Hu, Y. Wang, J. Xiang, Leaching behavior of vanadium from spent SCR catalyst and its immobilization in cement-based solidification/stabilization with sulfurizing agent, Fuel 243 (2019) 406–412, https://doi.org/10.1016/j.fuel.2019.01.160.
[139] L. De Windt, P. Chaurand, J. Rose, Kinetics of steel slag leaching: batch tests and modeling, Waste Manag. 31 (2011) 225–235, https://doi.org/10.1016/j.wasman.2010.05.018.
[140] H.A. van der Sloot, Characterization of the leaching behaviour of concrete mortars and of cement–stabilized wastes with different waste loading for long term environmental assessment, Waste Manag. 22 (2002) 181–186, https://doi.org/10.1016/s0956-053x(01)00067-8.
[141] S. Peysson, J. Péra, M. Chabannet, Immobilization of heavy metals by calcium sulfoaluminate cement, Cem. Concr. Res. 35 (2005) 2261–2270, https://doi.org/10.1016/j.cemconres.2005.03.015.
[142] A. Stumm, K. Garbev, G. Beuchle, L. Black, P. Stemmermann, R. Nüesch, Incorporation of zinc into calcium silicate hydrates, part I: formation of C-S-H(I) with C/S=2/3 and its isochemical counterpart gyrolite, Cem. Concr. Res. 35 (2005) 1665–1675, https://doi.org/10.1016/j.cemconres.2004.11.007.
[143] J. Rose, I. Moulin, J.-L. Hazemann, A. Masion, P.M. Bertsch, J.-Y. Bottero, F. Mosnier, C. Haehnel, X-ray absorption spectroscopy study of immobilization processes for heavy metals in calcium silicate hydrates: 1. Case of lead, Langmuir 16 (2000) 9900–9906, https://doi.org/10.1021/la0005208.
[144] A. Baldermann, V. Preissegger, S. Šimić, I. Letofsky-Papst, F. Mittermayr, M. Dietzel, Uptake of aqueous heavy metal ions (Co2+, Cu2+ and Zn2+) by calcium-aluminium-silicate-hydrate gels, Cem. Concr. Res. 147 (2021), 106521, https://doi.org/10.1016/j.cemconres.2021.106521.
[145] M.M. Ali, S.K. Agarwal, A. Pahuja, Potentials of copper slag utilisation in the manufacture of ordinary Portland cement, Adv. Cem. Res. 25 (2013) 208–216.
[146] L.E. García Medina, E. Orrantia Borunda, A. Aquilar Elguézabal, Uso de la escoria de cobre en el proceso de fabricación de clínker para cemento Portland, 2006.
[147] I. Vangelatos, G.N. Angelopoulos, D. Boufounos, Utilization of ferroalumina as raw material in the production of ordinary Portland cement, J. Hazard. Mater. 168 (2009) 473–478.
[148] S.A. Bernal, P.V. Krivenko, J.L. Provis, F. Puertas, W.D.A. Rickard, C. Shi, A. van Riessen, Other potential applications for alkali-activated materials, in: J.L. Provis, J.S.J. van Deventer (Eds.), Alkali Activated Materials: State-of-the-Art Report, RILEM TC 224-AAM, Springer Netherlands, Dordrecht, 2014, pp. 339–379.
[149] M. Giels, R.I. Iacobescu, V. Cappuyns, Y. Pontikes, J. Elsen, Understanding the leaching behavior of inorganic polymers made of iron rich slags, J. Clean. Prod. 238 (2019), 117736, https://doi.org/10.1016/j.jclepro.2019.117736.
[150] G.M.B. Mudd, V. David, The ever growing case for paste and thickened tailings – towards more sustainable mine waste management, AusIMM Bull. Geotech. Eng. (2013) 56–59.
[151] M. Gou, L. Zhou, N.W.Y. Then, Utilization of tailings in cement and concrete: a review, Sci. Eng. Compos. Mater. 26 (2019) 449–464, https://doi.org/10.1515/secm-2019-0029.
[152] N.P. Martins, S. Srivastava, F.V. Simão, H. Niu, P. Perumal, R. Snellings, M. Illikainen, H. Chambart, G. Habert, Exploring the potential for utilization of medium and highly sulfidic mine tailings in construction materials: a review, Sustainability 13 (2021) 12150.
[153] C. Siakati, A.P. Douvalis, P. Ziogas, A. Peys, Y. Pontikes, Impact of the solidification path of FeOx–SiO2 slags on the resultant inorganic polymers, J. Am. Ceram. Soc. 103 (2020) 2173–2184.
[154] A. Mancini, B. Lothenbach, G. Geng, D. Grolimund, D.F. Sanchez, S.C. Fakra, R. Dähn, B. Wehrli, E. Wieland, Iron speciation in blast furnace slag cements, Cem. Concr. Res. 140 (2021), 106287, https://doi.org/10.1016/j.cemconres.2020.106287.
[155] S.A. Bernal, V. Rose, J.L. Provis, The fate of iron in blast furnace slag particles during alkali-activation, Mater. Chem. Phys. 146 (2014) 1–5, https://doi.org/10.1016/j.matchemphys.2014.03.017.
[156] F.E. Furcas, B. Lothenbach, O.B. Isgor, S. Mundra, Z. Zhang, U.M. Angst, Solubility and speciation of iron in cementitious systems, Cem. Concr. Res. 151 (2022), 106620, https://doi.org/10.1016/j.cemconres.2021.106620.
[157] P.N. Lemougna, K.J.D. MacKenzie, G.N.L. Jameson, H. Rahier, U.F. Chinje Melo, The role of iron in the formation of inorganic polymers (geopolymers) from volcanic ash: a 57Fe Mössbauer spectroscopy study, J. Mater. Sci. 48 (2013) 5280–5286, https://doi.org/10.1007/s10853-013-7319-4.
[158] C. Liu, P.L. Lopez Gonzalez, S. Huang, Y. Pontikes, B. Blanpain, M. Guo, Experimental and mathematical simulation study on the granulation of a modified basic oxygen furnace steel slag, Metall. Mater. Trans. B 50 (2019) 1260–1268, https://doi.org/10.1007/s11663-019-01543-x.
[159] C. Liu, S. Huang, B. Blanpain, M. Guo, Effect of Al2O3 addition on mineralogical modification and crystallization kinetics of a high basicity BOF steel slag, Metall. Mater. Trans. B 50 (2019) 271–281, https://doi.org/10.1007/s11663-018-1465-7.
[160] Y. Pontikes, L. Machiels, S. Onisei, L. Pandelaers, D. Geysen, P.T. Jones, B. Blanpain, Slags with a high Al and fe content as precursors for inorganic polymers, Appl. Clay Sci. 73 (2013) 93–102, https://doi.org/10.1016/j.clay.2012.09.020.
[161] J. Van De Sande, A. Peys, T. Hertel, H. Rahier, Y. Pontikes, Upcycling of non-ferrous metallurgy slags: identifying the most reactive slag for inorganic polymer construction materials, Resour. Conserv. Recycl. 154 (2020), 104627.
[162] C. Siakati, A.P. Douvalis, A. Peys, Y. Pontikes, Binary, ternary and quaternary Fe-rich slags: Influence of Fe and Si substitution by Ca and Al on the atomic structure and reactivity, in: Proceedings of the 6th International Slag Valorisation Symposium, Mechelen, Belgium, 2019, pp. 325–328.
[163] M. Giels, T. Hertel, V. Hallet, Y. Pontikes, Designing highly reactive precursors from bauxite residue: can the RILEM R3 test assist?, in: Proceedings of the 7th International Slag Valorisation Symposium, Online, 2021, pp. 89–92.
[164] R.H. Bogue, Calculation of the compounds in Portland cement, Ind. Eng. Chem. Anal. Ed. 1 (1929) 192–197, https://doi.org/10.1021/ac50068a006.
[165] G.J. Redhammer, G. Tippelt, G. Roth, G. Amthauer, Structural variations in the brownmillerite series Ca2(Fe2–xAlx)O5: single-crystal X-ray diffraction at 25 °C and high-temperature X-ray powder diffraction (25 °C ≤ T ≤ 1000 °C), Am. Mineral. 89 (2004) 405–420, https://doi.org/10.2138/am-2004-2-322.
[166] L. Jiang, Y. Bao, Q. Yang, Y. Chen, G. Liu, F. Han, J. Wei, F. Engström, J. Deng, Formation of spinel phases in oxidized BOF slag under different cooling conditions, Steel Res. Int. 88 (2017), 1700066.
[167] D.E. Rogers, L.P. Aldridge, Hydrates of calcium ferrites and calcium aluminoferrites, Cem. Concr. Res. 7 (1977) 399–409, https://doi.org/10.1016/0008-8846(77)90068-0.
[168] A. Wesselsky, O.M. Jensen, Synthesis of pure Portland cement phases, Cem. Concr. Res. 39 (2009) 973–980, https://doi.org/10.1016/j.cemconres.2009.07.013.
[169] S. Ravaszová, K. Dvořák, Crystallization process in the preparation of the tetracalcium ferroaluminate, IOP Conf. Ser. Mater. Sci. Eng. 549 (2019), 012026, https://doi.org/10.1088/1757-899x/549/1/012026.
[170] T. Hanein, F.P. Glasser, M.N. Bannerman, Thermodynamic data for cement clinkering, Cem. Concr. Res. 132 (2020), 106043, https://doi.org/10.1016/j.cemconres.2020.106043.
[171] M. Selleby, An assessment of the ca-fe-O-si system, Metall. Mater. Trans. B 28 (1997) 577–596, https://doi.org/10.1007/s11663-997-0030-6.
[172] S. Ghazizadeh, T. Hanein, J.L. Provis, T. Matschei, Estimation of standard molar entropy of cement hydrates and clinker minerals, Cem. Concr. Res. 136 (2020), 106188, https://doi.org/10.1016/j.cemconres.2020.106188.
[175] G.W. Ward, Effect of heat treatment and cooling rate on the microscopic structure of Portland cement clinker, J. Res. Natl. Bur. Stand. 26 (1941) 49–64.
[176] R. Snellings, A. Bazzoni, K. Scrivener, The existence of amorphous phase in Portland cements: physical factors affecting Rietveld quantitative phase analysis, Cem. Concr. Res. 59 (2014) 139–146, https://doi.org/10.1016/j.cemconres.2014.03.002.

[177] M. Ichikawa, S. Ikeda, Y. Komukai, Effect of cooling rate and Na2O content on the character of the interstitial materials in portland cement clinker, Cem. Concr. Res. 24 (1994) 1092–1096, https://doi.org/10.1016/0008-8846(94)90033-7.

[178] B. Touzo, K.L. Scrivener, F.P. Glasser, Phase compositions and equilibria in the CaO–Al2O3–Fe2O3–SO3 system, for assemblages containing ye'elimite and ferrite Ca2(Al, Fe)O5, Cem. Concr. Res. 54 (2013) 77–86, https://doi.org/10.1016/j.cemconres.2013.08.005.

[179] A. Cuesta, I. Santacruz, S.G. Sanfélix, F. Fauth, M.A.G. Aranda, A.G. De la Torre, Hydration of C4AF in the presence of other phases: a synchrotron X-ray powder diffraction study, Constr. Build. Mater. 101 (2015) 818–827, https://doi.org/10.1016/j.conbuildmat.2015.10.114.

[180] S. Dolenec, K. Šter, M. Borštnar, K. Nagode, A. Ipavec, L. Žibret, Effect of the cooling regime on the mineralogy and reactivity of belite-sulfoaluminate clinkers, Minerals 10 (2020) 910.

[181] E.M. Gartner, J.F. Young, D. Damidot, I. Jawed, Hydration of Portland cement, in: P. Barnes, J. Bensted (Eds.), Structure and Performance of Cements, CRC Press, 2001, pp. 57–113.

[182] M. Murat, F. Sorrentino, Effect of large additions of Cd, Pb, Cr, Zn, to cement raw meal on the composition and the properties of the clinker and the cement, Cem. Concr. Res. 26 (1996) 377–385, https://doi.org/10.1016/S0008-8846(96)85025-3.

[183] T. Chabayashi, A. Nakamura, H. Kato, K. Sada, Effects of TiO2 and MgO on clinker mineral composition and cement physical characteristics, Cement Sci. Concr. Technol. 66 (2012) 211–216, https://doi.org/10.14250/cement.66.211.

[184] D. Shang, M. Wang, Z. Xia, S. Hu, F. Wang, Incorporation mechanism of titanium in Portland cement clinker and its effects on hydration properties, Constr. Build. Mater. 146 (2017) 344–349, https://doi.org/10.1016/j.conbuildmat.2017.03.129.

[185] G.K. Moir, F.P. Glasser, Mineralizers, modifiers, and activators in the clinkering process, in: Proceedings of the 9th International Congress on the Chemistry of Cement, New Delhi, India, 1992, p. 125.

[186] T.Y. Duvallet, T.L. Robl, F.P. Glasser, The effect of titanium dioxide on the structure and reactivity of ferrite, in: Proceedings of the 8th International Conference: Concrete in the Low Carbon Era, Dundee, UK, 2012, pp. 584–593.

[187] J. Neubauer, R. Sieber, H.J. Kuzel, M. Ecker, Investigations on introducing Si and Mg into Brownmillerite—a Rietveld refinement, Cem. Concr. Res. 26 (1996) 77–82, https://doi.org/10.1016/0008-8846(95)00178-6.

[188] T. Staněk, P. Sulovský, The impact of basic minor oxides on the clinker formation, Mater. Sci. Forum 908 (2017) 3–9, https://doi.org/10.4028/www.scientific.net/MSF.908.3.

[189] V.V. Timashev, The kinetics of clinker formation. The structure and composition of clinker and its phases, in: Proceedings of the 7th International Congress on the Chemistry of Cement, 1980, pp. 1–20.

[190] G. Malquori, V. Cirilli, The ferrite phase, in: Proceedings of the 3rd International Congress on the Chemistry of Cement, London, UK, 1952, pp. 120–136.

[191] T. Chabayashi, H. Nagata, A. Nakamura, H. Kato, Reduction of burning temperature of cement clinker by adjusting of mineral composition, Cement Sci. Concr. Technol. 66 (2012).

[192] K. Zhang, P. Shen, L. Yang, M. Rao, S. Nie, F. Wang, Development of high-ferrite cement: toward green cement production, J. Clean. Prod. 327 (2021), 129487, https://doi.org/10.1016/j.jclepro.2021.129487.

[193] D. Ariño Montoya, N. Pistofidis, G. Giannakopoulos, R.I. Iacobescu, M.S. Katsiotis, Y. Pontikes, Revisiting the iron-rich "ordinary Portland cement" towards valorisation of wastes: study of Fe-to-Al ratio on the clinker production and the hydration reaction, Mater. Struct. 54 (2021) 30, https://doi.org/10.1617/s11527-020-01601-w.

[194] W.V. Fernandes, S.M. Torres, C.A. Kirk, A.F. Leal, M.R. Lima Filho, D. Diniz, Incorporation of minor constituents into Portland cement tricalcium silicate: bond valence assessment of the alite M1 polymorph crystal structure using synchrotron XRPD data, Cem. Concr. Res. 136 (2020), 106125, https://doi.org/10.1016/j.cemconres.2020.106125.

[195] G.-C. Lai, T. Nojiri, K.-I. Nakano, Studies of the stability of β-Ca2SiO4 doped by minor ions, Cem. Concr. Res. 22 (1992) 743–754, https://doi.org/10.1016/0008-8846(92)90097-F.

[196] H.-Y. Yu, X.-L. Pan, B.-W. Liu, B. Wang, S.-W. Bi, Effect of iron oxides on activity of calcium aluminate clinker in CaO-Al2O3-SiO2 system, J. Iron Steel Res. Int. 21 (2014) 990–994, https://doi.org/10.1016/S1006-706X(14)60173-4.

[197] M. Selleby, An assessment of the Fe-O-Si system, Metall. Mater. Trans. B 28 (1997) 563–576.

[198] X. Huang, S. Hu, F. Wang, L. Yang, M. Rao, Y. Tao, Enhanced sulfate resistance: the importance of iron in aluminate hydrates, ACS Sustain. Chem. Eng. 7 (2019) 6792–6801, https://doi.org/10.1021/acssuschemeng.8b06097.

[199] P.J. Tikalsky, D. Roy, B. Scheetz, T. Krize, Redefining cement characteristics for sulfate-resistant Portland cement, Cem. Concr. Res. 32 (2002) 1239–1246, https://doi.org/10.1016/S0008-8846(02)00767-6.

[200] N. Noguchi, K. Siventhirarajah, T. Chabayashi, H. Kato, T. Nawa, Y. Elakneswaran, Hydration of ferrite-rich Portland cement: evaluation of Fe-hydrates and Fe uptake in calcium-silicate-hydrates, Constr. Build. Mater. 288 (2021), 123142.

[201] A. Mancini, E. Wieland, G. Geng, R. Dähn, J. Skibsted, B. Wehrli, B. Lothenbach, Fe(III) uptake by calcium silicate hydrates, Appl. Geochem. 113 (2020), 104460, https://doi.org/10.1016/j.apgeochem.2019.104460.

[202] G. Möschner, B. Lothenbach, F. Winnefeld, A. Ulrich, R. Figi, R. Kretzschmar, Solid solution between Al-ettringite and Fe-ettringite (Ca6[Al1−xFex(OH)6]2(SO4)3·26H2O), Cem. Concr. Res. 39 (2009) 482–489, https://doi.org/10.1016/j.cemconres.2009.03.001.

[203] B.Z. Dilnesa, B. Lothenbach, G. Renaudin, A. Wichser, E. Wieland, H. Jennings, Stability of monosulfate in the presence of iron, J. Am. Ceram. Soc. 95 (2012) 3305–3316, https://doi.org/10.1111/j.1551-2916.2012.05335.x.

[204] B.Z. Dilnesa, B. Lothenbach, G. Renaudin, A. Wichser, D. Kulik, Synthesis and characterization of hydrogarnet Ca3(AlxFe1−x)2(SiO4)y(OH)4(3−y), Cem. Concr. Res. 59 (2014) 96–111, https://doi.org/10.1016/j.cemconres.2014.02.001.

[205] B.Z. Dilnesa, B. Lothenbach, G. Le Saout, G. Renaudin, A. Mesbah, Y. Filinchuk, A. Wichser, E. Wieland, Iron in carbonate containing AFm phases, Cem. Concr. Res. 41 (2011) 311–323, https://doi.org/10.1016/j.cemconres.2010.11.017.

[206] G. Möschner, B. Lothenbach, J. Rose, A. Ulrich, R. Figi, R. Kretzschmar, Solubility of Fe–ettringite (Ca6[Fe(OH)6]2(SO4)3·26H2O), Geochim. Cosmochim. Acta 72 (2008) 1–18, https://doi.org/10.1016/j.gca.2007.09.035.

[207] B.Z. Dilnesa, E. Wieland, B. Lothenbach, R. Dähn, K.L. Scrivener, Fe-containing phases in hydrated cements, Cem. Concr. Res. 58 (2014) 45–55, https://doi.org/10.1016/j.cemconres.2013.12.012.

[208] M. Vespa, E. Wieland, R. Dähn, B. Lothenbach, Identification of the thermodynamically stable Fe-containing phase in aged cement pastes, J. Am. Ceram. Soc. 98 (2015) 2286–2294, https://doi.org/10.1111/jace.13542.

[209] F.J. Tang, E.M. Gartner, Influence of sulfate source on Portland cement hydration, in: PCE R&D Serial No. 1876, Construction Technology Laboratories, Inc, Skokie, Illinois, USA, 1987.

[210] K. Zhang, P. Shen, L. Yang, M. Rao, F. Wang, Improvement of the hydration kinetics of high ferrite cement: synergic effect of gypsum and C3S–C4AF systems, ACS Sustain. Chem. Eng. 9 (2021) 15127–15137, https://doi.org/10.1021/acssuschemeng.1c02323.

[211] B. Lothenbach, G. Le Saout, E. Gallucci, K. Scrivener, Influence of limestone on the hydration of Portland cements, Cem. Concr. Res. 38 (2008) 848–860, https://doi.org/10.1016/j.cemconres.2008.01.002.

[212] E. Gartner, D. Myers, Influence of tertiary alkanolamines on Portland cement hydration, J. Am. Ceram. Soc. 76 (1993) 1521–1530, https://doi.org/10.1111/j.1151-2916.1993.tb03934.x.

[213] Z. Lu X. Kong D. Jansen C. Zhang A comparative study of the effects of two alkanolamines on cement hydration. Adv. Cem. Res. 0, 1-10, doi:10.1680/jadcr.20.00063.

[214] T. Hanein, J.-L. Galvez-Martos, M.N. Bannerman, Carbon footprint of calcium sulfoaluminate clinker production, J. Clean. Prod. 172 (2018) 2278–2287, https://doi.org/10.1016/j.jclepro.2017.11.183.

[215] F. Bullerjahn, T. Scholten, K.L. Scrivener, M.B. Haha, A. Wolter, Formation, composition and stability of ye'elimite and iron-bearing solid solutions, Cem. Concr. Res. 131 (2020), 106009.

[216] J.S. Ndzila, S. Liu, G. Jing, S. Wang, Z. Ye, The effect of Fe3+ ion substitution on the crystal structure of Ye'elimite, Ceramics-Silikáty 64 (2020) 18–28.

[217] X. Yao, S. Yang, H. Dong, S. Wu, X. Liang, W. Wang, Effect of CaO content in raw material on the mineral composition of ferric-rich sulfoaluminate clinker, Constr. Build. Mater. 263 (2020), https://doi.org/10.1016/j.conbuildmat.2020.120431.

[218] M. Idrissi, A. Diouri, D. Damidot, J.M. Greneche, M.A. Talbi, M. Taibi, Characterisation of iron inclusion during the formation of calcium sulfoaluminate phase, Cem. Concr. Res. 40 (2010) 1314–1319, https://doi.org/10.1016/j.cemconres.2010.02.009.

[219] Y. Huang, Y. Pei, J. Qian, X. Gao, J. Liang, G. Duan, P. Zhao, L. Lu, X. Cheng, Bauxite free iron rich calcium sulfoaluminate cement: preparation, hydration and properties, Constr. Build. Mater. 249 (2020), 118774, https://doi.org/10.1016/j.conbuildmat.2020.118774.

[220] F. Bullerjahn, M. Zajac, M.B. Haha, K.L. Scrivener, Factors influencing the hydration kinetics of ye'elimite; effect of mayenite, Cem. Concr. Res. 116 (2019) 113–119.

[221] E. Gartner, T. Sui, Alternative cement clinkers, Cem. Concr. Res. 114 (2018) 27–39, https://doi.org/10.1016/j.cemconres.2017.02.002.

[222] V. Morin, P. Termkhajornkit, B. Huet, G. Pham, Impact of quantity of anhydrite, water to binder ratio, fineness on kinetics and phase assemblage of belite-ye'elimite-ferrite cement, Cem. Concr. Res. 99 (2017) 8–17.

[223] A.J.M. Cuberos, A.G. De la Torre, G. Alvarez-Pinazo, M.C. Martín-Sedeño, K. Schollbach, H. Pöllmann, M.A.G. Aranda, Active iron-rich belite sulfoaluminate cements: clinkering and hydration, Environ. Sci. Technol. 44 (2010) 6855–6862.

[224] G.M. Fortes, R.R. Lourenço, M. Montini, J.B. Gallo, J.D.A. Rodrigues, Synthesis and mechanical characterization of iron oxide rich sulfobelite cements prepared using bauxite residue, Mater. Res. 19 (2016) 276–284, https://doi.org/10.1590/1980-5373-MR-2015-0180.

[225] T. Hanein, T.Y. Duvallet, R.B. Jewell, A.E. Oberlink, T.L. Robl, Y. Zhou, F. P. Glasser, M.N. Bannerman, Alite calcium sulfoaluminate cement: chemistry and thermodynamics, Adv. Cem. Res. 31 (2019) 94–105.

[226] J.D. Zea-Garcia, I. Santacruz, M.A.G. Aranda, G. Angeles, Alite-belite-ye'elimite cements: effect of dopants on the clinker phase composition and properties, Cem. Concr. Res. 115 (2019) 192–202.

[227] T.Y. Duvallet, Influence of Ferrite Phase in Alite-calcium Sulfoaluminate Cements, 2014.

[228] D. Londono-Zuluaga, J.I. Tobon, M.A.G. Aranda, I. Santacruz, A.G. De la Torre, Clinkering and hydration of belite-alite-ye′elimite cement, Cem. Concr. Compos. 80 (2017) 333–341.

[229] V. Isteri, K. Ohenoja, T. Hanein, H. Kinoshita, M. Illikainen, P. Tanskanen, T. Fabritius, The effect of fluoride and iron content on the clinkering of Alite-Ye'elimite-Ferrite (AYF) cement systems, Front. Built Environ. (2021) 7, https://doi.org/10.3389/fbuil.2021.698830.

[230] M.A. Khairul, J. Zanganeh, B. Moghtaderi, The composition, recycling and utilisation of Bayer red mud, Resour. Conserv. Recycl. 141 (2019) 483–498.

[231] M.M. Ali, S.K. Agarwal, A. Pahuja, B.K. Singh, S. Duggal, Utilisation of by-product jarosite in the manufacture of ordinary Portland cement, Adv. Cem. Res. 26 (2014) 41–51.
[232] P.E. Tsakiridis, S. Agatzini-Leonardou, P. Oustadakis, M. Katsioti, E. Mauridou, Examination of the jarosite–alunite precipitate addition in the raw meal for the production of Portland cement clinker, Cem. Concr. Res. 35 (2005) 2066–2073.
[233] M. Katsioti, P.E. Tsakiridis, S. Agatzini-Leonardou, P. Oustadakis, Examination of the jarosite–alunite precipitate addition in the raw meal for the production of Portland and sulfoaluminate-based cement clinkers, Int. J. Miner. Process. 76 (2005) 217–224.
[234] J.H. Ideker, K. Scrivener, H. Fryda, B. Touzo, Calcium aluminate cements, in: P. Hewlett, M. Liska (Eds.), Lea's Chemicstry of Cement and Concrete, Butterworth-Heinemann, 2019.
[235] H. Pöllmann, Calcium aluminate cements – raw materials, differences, hydration and properties, Rev. Mineral. Geochem. 74 (2012) 1–82, https://doi.org/10.2138/rmg.2012.74.1.
[236] G. Le Saout, Phase assemblage in calcium aluminate cements: a review, ALITinform 2 (2018) 12–20.
[237] H.G. Midgley, The composition of pleochroite in high alumina cement clinker, Cem. Concr. Res. 9 (1979) 623–630, https://doi.org/10.1016/0008-8846(79)90147-9.
[238] J. Goergens, T. Manninger, F. Goetz-Neunhoeffer, In-situ XRD study of the temperature-dependent early hydration of calcium aluminate cement in a mix with calcite, Cem. Concr. Res. 136 (2020), 106160, https://doi.org/10.1016/j.cemconres.2020.106160.
[239] S. Pamenter, R.J. Myers, Decarbonizing the cementitious materials cycle: a whole-systems review of measures to decarbonize the cement supply chain in the UK and European contexts, J. Ind. Ecol. 25 (2021) 359–376, https://doi.org/10.1111/jiec.13105.
[240] R. Snellings, G. Mertens, J. Elsen, Supplementary cementitious materials, Rev. Mineral. Geochem. 74 (2012) 211–278, https://doi.org/10.2138/rmg.2012.74.6.
[241] M.C. Juenger, R. Snellings, S.A. Bernal, Supplementary cementitious materials: new sources, characterization, and performance insights, Cem. Concr. Res. 122 (2019) 257–273.
[243] World Steel Association, Climate change and the production of iron and steel, Available online: https://www.worldsteel.org/publications/position-papers/climate-change-policy-paper.html.
[244] F. Avet, R. Snellings, A.A. Diaz, M.B. Haha, K. Scrivener, Development of a new rapid, relevant and reliable (R3) test method to evaluate the pozzolanic reactivity of calcined kaolinitic clays, Cem. Concr. Res. 85 (2016) 1–11.
[245] R. Snellings, X. Li, F. Avet, K. Scrivener, Rapid, robust, and relevant (R3) reactivity test for supplementary cementitious materials, ACI Mater. J. 116 (2019).
[246] F. Zunino, M. Lopez, Decoupling the physical and chemical effects of supplementary cementitious materials on strength and permeability: a multi-level approach, Cem. Concr. Compos. 65 (2016) 19–28, https://doi.org/10.1016/j.cemconcomp.2015.10.003.
[247] C.M. Tibbetts, J.M. Paris, C.C. Ferraro, K.A. Riding, T.G. Townsend, Relating water permeability to electrical resistivity and chloride penetrability of concrete containing different supplementary cementitious materials, Cem. Concr. Compos. 107 (2020), 103491, https://doi.org/10.1016/j.cemconcomp.2019.103491.
[248] M. Thomas, The effect of supplementary cementing materials on alkali-silica reaction: a review, Cem. Concr. Res. 41 (2011) 1224–1231, https://doi.org/10.1016/j.cemconres.2010.11.003.
[249] M.J. Tapas, L. Sofia, K. Vessalas, P. Thomas, V. Sirivivatnanon, K. Scrivener, Efficacy of SCMs to mitigate ASR in systems with higher alkali contents assessed by pore solution method, Cem. Concr. Res. 142 (2021), 106353, https://doi.org/10.1016/j.cemconres.2021.106353.
[250] T. Chappex, K.L. Scrivener, H. Jennings, The effect of aluminum in solution on the dissolution of amorphous silica and its relation to cementitious systems, J. Am. Ceram. Soc. (2012), https://doi.org/10.1111/jace.12098 n/a-n/a.
[251] T. Chappex, K.L. Scrivener, The influence of aluminium on the dissolution of amorphous silica and its relation to alkali silica reaction, Cem. Concr. Res. 42 (2012) 1645–1649, https://doi.org/10.1016/j.cemconres.2012.09.009.
[252] M.I. Sanchez de Rojas, J. Rivera, M. Frias, F. Marin, Use of recycled copper slag for blended cements, J. Chem. Technol. Biotechnol. 83 (2008) 209–217.
[253] R.S. Edwin, M. De Schepper, E. Gruyaert, N. De Belie, Effect of secondary copper slag as cementitious material in ultra-high performance mortar, Constr. Build. Mater. 119 (2016) 31–44, https://doi.org/10.1016/j.conbuildmat.2016.05.007.
[254] A. Mancini, E. Wieland, G. Geng, B. Lothenbach, B. Wehrli, R. Dähn, Fe(II) interaction with cement phases: method development, wet chemical studies and X-ray absorption spectroscopy, J. Colloid Interface Sci. 588 (2021) 692–704, https://doi.org/10.1016/j.jcis.2020.11.085.
[255] A. Peys, L. Arnout, B. Blanpain, H. Rahier, K. Van Acker, Y. Pontikes, Mix-design parameters and real-life considerations in the pursuit of lower environmental impact inorganic polymers, Waste Biomass Valorization 9 (2018) 879–889, https://doi.org/10.1007/s12649-017-9877-1.
[256] A. Mellado, C. Catalán, N. Bouzón, M.V. Borrachero, J.M. Monzó, J. Payá, Carbon footprint of geopolymeric mortar: study of the contribution of the alkaline activating solution and assessment of an alternative route, RSC Adv. 4 (2014) 23846–23852, https://doi.org/10.1039/C4RA03375B.
[257] A. Heath, K. Paine, M. McManus, Minimising the global warming potential of clay based geopolymers, J. Clean. Prod. 78 (2014) 75–83, https://doi.org/10.1016/j.jclepro.2014.04.046.
[258] G. Habert, C. Ouellet-Plamondon, Recent update on the environmental impact of geopolymers, RILEM Tech. Lett. 1 (2016), https://doi.org/10.21809/rilemtechlett.2016.6.
[259] B.C. McLellan, R.P. Williams, J. Lay, A. van Riessen, G.D. Corder, Costs and carbon emissions for geopolymer pastes in comparison to ordinary Portland cement, J. Clean. Prod. 19 (2011) 1080–1090, https://doi.org/10.1016/j.jclepro.2011.02.010.
[260] J.L. Provis, Alkali-activated materials, Cem. Concr. Res. 114 (2018) 40–48.
[261] V. Ponomar, J. Yliniemi, E. Adesanya, K. Ohenoja, M. Illikainen, An overview of the utilisation of Fe-rich residues in alkali-activated binders: Mechanical properties and state of iron, J. Clean. Prod. 330 (2022), 129900, https://doi.org/10.1016/j.jclepro.2021.129900.
[262] H. Rahier, B. Van Mele, M. Biesemans, J. Wastiels, X. Wu, Low-temperature synthesized aluminosilicate glasses, J. Mater. Sci. 31 (1996) 71–79, https://doi.org/10.1007/BF00355128.
[263] J. Davidovits, Geopolymers and geopolymeric materials, J. Therm. Anal. 35 (1989) 429–441, https://doi.org/10.1007/Bf01904446.
[264] P. Duxson, A. Fernández-Jiménez, J.L. Provis, G.C. Lukey, A. Palomo, J.S.J. van Deventer, Geopolymer technology: the current state of the art, J. Mater. Sci. 42 (2007) 2917–2933, https://doi.org/10.1007/s10853-006-0637-z.
[265] B. Walkley, R. San Nicolas, M.-A. Sani, G.J. Rees, J.V. Hanna, J.S.J. van Deventer, J.L. Provis, Phase evolution of C-(N)-A-S-H/N-A-S-H gel blends investigated via alkali-activation of synthetic calcium aluminosilicate precursors, Cem. Concr. Res. 89 (2016) 120–135, https://doi.org/10.1016/j.cemconres.2016.08.010.
[266] S.A. Bernal, J.L. Provis, B. Walkley, R. San Nicolas, J.D. Gehman, D.G. Brice, A. R. Kilcullen, P. Duxson, J.S.J. van Deventer, Gel nanostructure in alkali-activated binders based on slag and fly ash, and effects of accelerated carbonation, Cem. Concr. Res. 53 (2013) 127–144, https://doi.org/10.1016/j.cemconres.2013.06.007.
[267] R. Tänzer, A. Buchwald, D. Stephan, Effect of slag chemistry on the hydration of alkali-activated blast-furnace slag, Mater. Struct. 48 (2015) 629–641, https://doi.org/10.1617/s11527-014-0461-x.
[268] C.E. White, L.L. Daemen, M. Hartl, K. Page, Intrinsic differences in atomic ordering of calcium (alumino)silicate hydrates in conventional and alkali-activated cements, Cem. Concr. Res. 67 (2015) 66–73, https://doi.org/10.1016/j.cemconres.2014.08.006.
[269] M.B. Haha, B. Lothenbach, G. Le Saout, F. Winnefeld, Influence of slag chemistry on the hydration of alkali-activated blast-furnace slag — Part I: effect of MgO, Cem. Concr. Res. 41 (2011) 955–963, https://doi.org/10.1016/j.cemconres.2011.05.002.
[270] M.B. Haha, B. Lothenbach, G. Le Saout, F. Winnefeld, Influence of slag chemistry on the hydration of alkali-activated blast-furnace slag — Part II: effect of Al2O3, Cem. Concr. Res. 42 (2012) 74–83, https://doi.org/10.1016/j.cemconres.2011.08.005.
[271] A. Peys, A.P. Douvalis, V. Hallet, H. Rahier, B. Blanpain, Y. Pontikes, Inorganic polymers from CaO-FeOx-SiO2 slag: the start of oxidation of Fe and the formation of a mixed valence binder, Front. Mater. 6 (2019) 212.
[272] L. Machiels, L. Arnout, P.T. Jones, B. Blanpain, Y. Pontikes, in: Fe-Si-glasses as Geopolymer Precursors: Decreasing the Amount of Activating Solution, 2013, pp. 303–306.
[273] I. Maragkos, I.P. Giannopoulou, D. Panias, Synthesis of ferronickel slag-based geopolymers, Miner. Eng. 22 (2009) 196–203, https://doi.org/10.1016/j.mineng.2008.07.003.
[274] S. Onisei, K. Lesage, B. Blanpain, Y. Pontikes, Early age microstructural transformations of an inorganic polymer made of fayalite slag, J. Am. Ceram. Soc. 98 (2015) 2269–2277, https://doi.org/10.1111/jace.13548.
[275] J. Denissen, L. Kriskova, Y. Pontikes, Kinetics of pore formation and resulting properties of lightweight inorganic polymers, J. Am. Ceram. Soc. 102 (2019) 3940–3950, https://doi.org/10.1111/jace.16301.
[276] V. Hallet, A. Peys, A. Katsiki, H. Rahier, S. Onisei, Y. Pontikes, The influence of activating solution on the kinetics and compressive strength of an iron-rich slag paste, in: Proceedings of the 5th International Slag Valorisation Symposium, Leuven, Belgium, 3-5 April, 2017, pp. 357–360.
[277] C. Siakati, A.P. Douvalis, P. Ziogas, A. Peys, Y. Pontikes, Impact of the solidification path of FeOx-SiO2 slags on the resultant inorganic polymers, J. Am. Ceram. Soc. 103 (2019) 2173–2184, https://doi.org/10.1111/jace.16869.
[278] G. Beersaerts, A. Vananroye, D. Sakellariou, C. Clasen, Y. Pontikes, Rheology of an alkali-activated Fe-rich slag suspension: identifying the impact of the activator chemistry and slag particle interactions, J. Non-Cryst. Solids 561 (2021), 120747, https://doi.org/10.1016/j.jnoncrysol.2021.120747.
[279] M. Albitar, M.S. Mohamed Ali, P. Visintin, M. Drechsler, Effect of granulated lead smelter slag on strength of fly ash-based geopolymer concrete, Constr. Build. Mater. 83 (2015) 128–135, https://doi.org/10.1016/j.conbuildmat.2015.03.009.
[280] M. Xia, F. Muhammad, L. Zeng, S. Li, X. Huang, B. Jiao, Y. Shiau, D. Li, Solidification/stabilization of lead-zinc smelting slag in composite based geopolymer, J. Clean. Prod. 209 (2019) 1206–1215, https://doi.org/10.1016/j.jclepro.2018.10.265.
[281] J. Van De Sande, A. Peys, T. Hertel, S. Onisei, B. Blanpain, Y. Pontikes, Glass Forming Ability of Slags in the FeOx-SiO2-CaO System and Properties of the Inorganic Polymers Made Thereof, 2017.
[282] L. Kriskova, L. Machiels, Y. Pontikes, Inorganic polymers from a plasma convertor slag: effect of activating solution on microstructure and properties, J. Sustain. Metall. 1 (2015) 240–251.
[283] A.M. Kalinkin, S. Kumar, B.I. Gurevich, T.C. Alex, E.V. Kalinkina, V. V. Tyukavkina, V.T. Kalinnikov, R. Kumar, Geopolymerization behavior of Cu–Ni

slag mechanically activated in air and in CO2 atmosphere, Int. J. Miner. Process. 112–113 (2012) 101–106, https://doi.org/10.1016/j.minpro.2012.05.001.
[284] K. Gong, A. Peys, Y. Pontikes, C. White, Alkali-activated Fe-rich slag with superior resistance to MgSO4 attack, in: Proceedings of the 9th Advances in Cement Based Materials (American Ceramic Society Cements Division), 2018.
[285] L. Arnout, W. Crijns, Y. Diquelou, J. Plas, J. Huybrechts, L. Cuyvers, D. Delaere, N. D. Belie, Y. Pontikes, J. Spinnewyn, Industrial validation of alkali-activated slag concrete in agricultural environments, in: Proceedings of the 7th International Slag Valorisation Symposium, Online, 27-29 April, 2021, p. 58.
[286] K. Sakkas, P. Nomikos, A. Sofianos, D. Panias, Sodium-based fire resistant geopolymer for passive fire protection, Fire Mater. 39 (2015) 259–270, https://doi.org/10.1002/fam.2244.
[287] J.L. Provis, K. Arbi, S.A. Bernal, D. Bondar, A. Buchwald, A. Castel, S. Chithiraputhiran, M. Cyr, A. Dehghan, K. Dombrowski-Daube, et al., RILEM TC 247-DTA round robin test: mix design and reproducibility of compressive strength of alkali-activated concretes, Mater. Struct. 52 (2019) 99, https://doi.org/10.1617/s11527-019-1396-z.
[288] G.J.G. Gluth, K. Arbi, S.A. Bernal, D. Bondar, A. Castel, S. Chithiraputhiran, A. Dehghan, K. Dombrowski-Daube, A. Dubey, V. Ducman, et al., RILEM TC 247-DTA round robin test: carbonation and chloride penetration testing of alkali-activated concretes, Mater. Struct. 53 (2020) 21, https://doi.org/10.1617/s11527-020-1449-3.
[289] F. Winnefeld, G.J.G. Gluth, S.A. Bernal, M.C. Bignozzi, L. Carabba, S. Chithiraputhiran, A. Dehghan, S. Dolenec, K. Dombrowski-Daube, A. Dubey, et al., RILEM TC 247-DTA round robin test: sulfate resistance, alkali-silica reaction and freeze–thaw resistance of alkali-activated concretes, Mater. Struct. 53 (2020) 140, https://doi.org/10.1617/s11527-020-01562-0.
[290] J.L. Provis, D.G. Brice, A. Buchwald, P. Duxson, E. Kavalerova, P.V. Krivenko, C. Shi, J.S.J.V. Deventer, J.A.L.M. Wiercx, Demonstration projects and applications in building and civil infrastructure, in: J.L. Provis, J.S.J.V. Deventer (Eds.), Alkali Activated Materials: State-of-the-Art Report, RILEM TC 224-AAM Volume 13, Springer, 2014, pp. 309–338.
[291] A. Katsiki, T. Hertel, T. Tysmans, Y. Pontikes, H. Rahier, Metakaolinite phosphate cementitious matrix: inorganic polymer obtained by acidic activation, Materials 12 (2019) 442.
[292] A. Katsiki, A. Peys, Y. Pontikes, H. Rahier, Activation of fayalite slag towards inorganic polymers, in: Proceedings of the 5th International Slag Valorisation Symposium, Leuven, Belgium, April 2017, 2017.
[293] S.-Y. Pan, Y.-H. Chen, L.-S. Fan, H. Kim, X. Gao, T.-C. Ling, P.-C. Chiang, S.-L. Pei, G. Gu, CO2 mineralization and utilization by alkaline solid wastes for potential carbon reduction, Nat. Sustain. 3 (2020) 399–405, https://doi.org/10.1038/s41893-020-0486-9.
[294] C.M. Woodall, N. McQueen, H. Pilorgé, J. Wilcox, Utilization of mineral carbonation products: current state and potential, Greenhouse Gases Sci. Technol. 9 (2019) 1096–1113, https://doi.org/10.1002/ghg.1940.
[295] M. Quaghebeur, P. Nielsen, L. Horckmans, D. Van Mechelen, Accelerated carbonation of steel slag compacts: development of high-strength construction materials, Front. Energy Res. 3 (2015) 12, https://doi.org/10.3389/fenrg.2015.00052.
[296] P. Nielsen, M.A. Boone, L. Horckmans, R. Snellings, M. Quaghebeur, Accelerated carbonation of steel slag monoliths at low CO2 pressure – microstructure and strength development, J. CO_2 Util. 36 (2020) 124–134, https://doi.org/10.1016/j.jcou.2019.10.022.
[297] S. Srivastava, R. Snellings, V. Meynen, P. Cool, Utilising the principles of FeCO3 scaling for cementation in H2O-CO2(g)-Fe system, Corros. Sci. 169 (2020), https://doi.org/10.1016/j.corsci.2020.108613.
[298] S. Srivastava, R. Snellings, V. Meynen, P. Cool, Siderite-calcite (FeCO3–CaCO3) series cement formation by accelerated carbonation of CO2(g)–H2O–Fe–Ca(OH)2 systems, Cem. Concr. Compos. 122 (2021), 104137, https://doi.org/10.1016/j.cemconcomp.2021.104137.
[299] M.D. Jackson, E.N. Landis, P.F. Brune, M. Vitti, H. Chen, Q. Li, M. Kunz, H.-R. Wenk, P.J.M. Monteiro, A.R. Ingraffea, Mechanical resilience and cementitious processes in Imperial Roman architectural mortar, Proc. Natl. Acad. Sci. 111 (2014) 18484–18489, https://doi.org/10.1073/pnas.1417456111.
[300] J. MacFarlane, T. Vanorio, P.J.M. Monteiro, Multi-scale imaging, strength and permeability measurements: understanding the durability of Roman marine concrete, Constr. Build. Mater. 272 (2021), 121812, https://doi.org/10.1016/j.conbuildmat.2020.121812.
[301] M. Chabannes, E. Garcia-Diaz, L. Clerc, J.-C. Bénézet, Effect of curing conditions and Ca(OH)2-treated aggregates on mechanical properties of rice husk and hemp concretes using a lime-based binder, Constr. Build. Mater. 102 (2016) 821–833, https://doi.org/10.1016/j.conbuildmat.2015.10.206.
[302] T. Hanein, M. Simoni, C.L. Woo, J.L. Provis, H. Kinoshita, Decarbonisation of calcium carbonate at atmospheric temperatures and pressures, with simultaneous CO2 capture, through production of sodium carbonate, Energ. Environ. Sci. 14 (12) (2021) 6595–6604.
[303] L.D. Ellis, A.F. Badel, M.L. Chiang, R.J.Y. Park, Y.M. Chiang, Toward electrochemical synthesis of cement—an electrolyzer-based process for decarbonating CaCO3 while producing useful gas streams, Proc. Natl. Acad. Sci. 117 (23) (2020) 12584–12591.